LYRA Calibration Methods: New Channels

IED, 25 Oct 2006
rev. 21 Sep 2007 (additional sample spectra)
rev. 07 Apr 2008 (updated responsivities)
rev. 18 Jul 2008 (new spectra, incl. SORCE)
rev. **16 Jun 2009** (updated responsivities, new channels)

In an earlier report (*IED_20060818_LYRA_Radiometric.pdf*), it was considered how to calculate the solar signal (in absolute physical units, e.g., W m-2) from its corresponding LYRA channel output (e.g., converted to A). It was argued that this estimation must involve the (potentially variable) purity, the (constant) aperture size, and a factor (linear or else) that combines the integrals of filter transmittance and detector responsivity in the spectral interval of interest.

Simulations showed the following: For the Lyman-alpha channels (*-1), purity grows with irradiance. For the Herzberg channels (*-2), purities and resulting calibration factors appear to be constant. For the Aluminium channels (*-3), purity varies heavily with irradiance. For the Zirconium channels (*-4), purity appears to be constant but responsivity grows with irradiance. - In this **update**, the Zr channel was redefined to be 6 – 20 nm; thus it behaves in a way similar to the Al channel.

The question was asked if one could use the LYRA channel signal itself to calculate calibration factors that depend on the signal strength, maybe in a non-linear way. This was discussed at the LYRA meeting in Davos (05/06 Oct 2006) on the basis of the information shown in an earlier version of Figure 0 (see next page). It was suggested to try and use information from *other* LYRA channels instead, in order to enhance the purity of certain problematic channels. In particular, it is clearly visible from the spectral responsivities of the Lyman-alpha channels that they are influenced by the neighbouring longer-wavelength continuum around 180-230 nm. Likewise, it is visible that the spectral responsivities of the Aluminium channels are influenced by the neighbouring shorter-wavelength signals around 1-10 nm. Since these disturbing signals are in fact observed and measured by LYRA via the Herzberg and Zirconium channels, respectively, it was suggested to subtract these signals in an appropriate way.

In the following, an attempt is suggested for procedures and resulting software for all twelve LYRA channels. First, in Figures 1-1 etc., the measured combined responsivity is graphically presented for each channel together with seven simulated spectral output signals. These signals were simulated with the help of TIMED/SEE spectral data sets called “min”, “high”, “max”, “pre1”, “fla1”, “pre2”, and “fla2”, taken on different days and representing a variety of solar irradiances to be expected. A longer-wavelength extension concerning wavelengths above ~200 nm was added to the TIMED/SEE data sets; this extension does not vary. (Please note **Update** next page!) Nominal intervals are marked in red.- Below these figures, the simulated values for the LYRA end signals are shown in a table: the “total” expected output signal, the “pure” signal of interest (defined by the nominal spectral interval of the channel), and the resulting “residual” difference signal (all in nA), together with the “solar” signal, i.e. the integrated input from the TIMED/SEE interval of interest (in W m-2). - Subsequently, methods are suggested to calculate the latter from the former.

The procedures suggested here are solely based on the seven data sets mentioned above. The initial assumption that zero solar input should lead to zero LYRA output has been dropped. As soon as the assumed models look “reasonable”, linear interpolation between data points is suggested (channels *-3 and *-4) instead of assuming higher-order polynomial or exponential functions in the case of sublinear or superlinear relations. In the other cases, simple polynomials can be used (channels *-1 and *-2).

Figures 1-1a etc. show the relations between total or pure LYRA signals to the solar signal in the upper row, as well as the relation between the channel signal or – where applicable – the neighbouring channel signal and the residual signal in the lower row. The arguments are similar for all three heads (only the numerical values vary),

but different for all four channels.

In the case of higher values in the Aluminium channels (*-3), where more than 90% contamination have to be estimated and subtracted, the success appears doubtful, and the initial approach may be suggested, namely, using the signal of the channel itself (instead of the neighbouring channel) to deduce the pure signal.

The seven TIMED/SEE samples initially used for the simulations were the following:

min	24 Feb 2005	solar minimum
high	11 Nov 2003	high solar flux
max	28 Oct 2003	solar maximum
pre1	28 Oct 2003	before X17 flare
fla1	28 Oct 2003	briefly after X17 flare
pre2	03 Nov 2003	before X3.9 flare
fla2	03 Nov 2003	briefly after X3.9 flare

According to the SEE instrument paper *(http://lasp.colorado.edu/see/documents/SEE_Instr_Paper.pdf)* these observations are "modeled" below 25 nm. - For the wavelength range above 193 nm up to 1000 nm, initially spectral values from another source were added, identically for all seven samples.

Update (18 Jul 2008):
After communication with the team from TIMED/SEE and SORCE, a new set of solar sample spectra was constructed. Apparently, the above-mentioned samples high and max had been largely over-estimated, especially in the very short wavelengths, while the sample min had been underestimated.

- Since the time when the input for the LYRA Radiometric Model was first constructed (2005), TIMED/SEE spectra have been recalibrated, currently using data products version 9.
- Additionally, it was suggested to use SORCE spectra for the longer wavelength part (i.e. above 116 nm).
- Since solar irradiance generally decreased during the last years, a new minimum could be selected and used from end-June 2008.
- The advantages are: Hopefully more realistically expected variations; a set of actually differing spectra for the Herzberg channels and the NUV-VIS-IR extension; in the end, smoother calibration curves result.

The seven samples now used for the simulations are the following (1 nm – 116 nm taken from TIMED/SEE, 116 nm – 2400 nm taken from various SORCE instruments):

omin	24 Feb 2005	(old) solar minimum
ohig	11 Nov 2003	(old) high solar flux
nmin	29 Jun 2008	(new) solar minimum
pre1	28 Oct 2003	before X17 flare
fla1	28 Oct 2003	briefly after X17 flare
pre2	03 Nov 2003	before X3.9 flare
fla2	03 Nov 2003	briefly after X3.9 flare

The TIMED/SEE part of pre1, fla1, pre2, fla2 is unchanged. The SORCE parts for pre1 and fla1 (as well as for pre2 and fla2) are identical, since SORCE only offers observations on a daily basis, while TIMED/SEE offers several (~14) observations per day. The old "max" sample spectrum is deleted, since it is covered by fla1. Spectrum nmin is introduced to cover the current solar minimum. Samples omin and ohig include the most recently calibrated TIMED/SEE spectra for the "old" dates.

Update (16 Jun 2009):

Apart from the re-definition of the Zr channel, improved responsivities were provided by ABM, and four "virtual" new channels were introduced.

- Channel *-5 simulates the expected output of SWAP (17.5 nm) with the help of LYRA channel *-3.
- Channel *-6 does the same with LYRA channel *-4.
- Channel *-7 simulates the expected output of the short-wavelength contamination of LYRA channel *-3 (< 5 nm).
- Channel *-8 does the same with LYRA channel *-4 (< 2 nm).

These additional channels will be used for cross-calibration with SWAP and TIMED/SEE. If successful, the short-wavelength channels might also be used for producing additional time series.

Finally, the lowest spectral entry of TIMED/SEE, representing the interval below 1 nm, was included in the LYRA estimate, using the LYRA responsivity measured at 1 nm. This increases the estimated total signal and reduces purities for all channels except *-1 and *-2 which are not responsive for very short wavelengths.

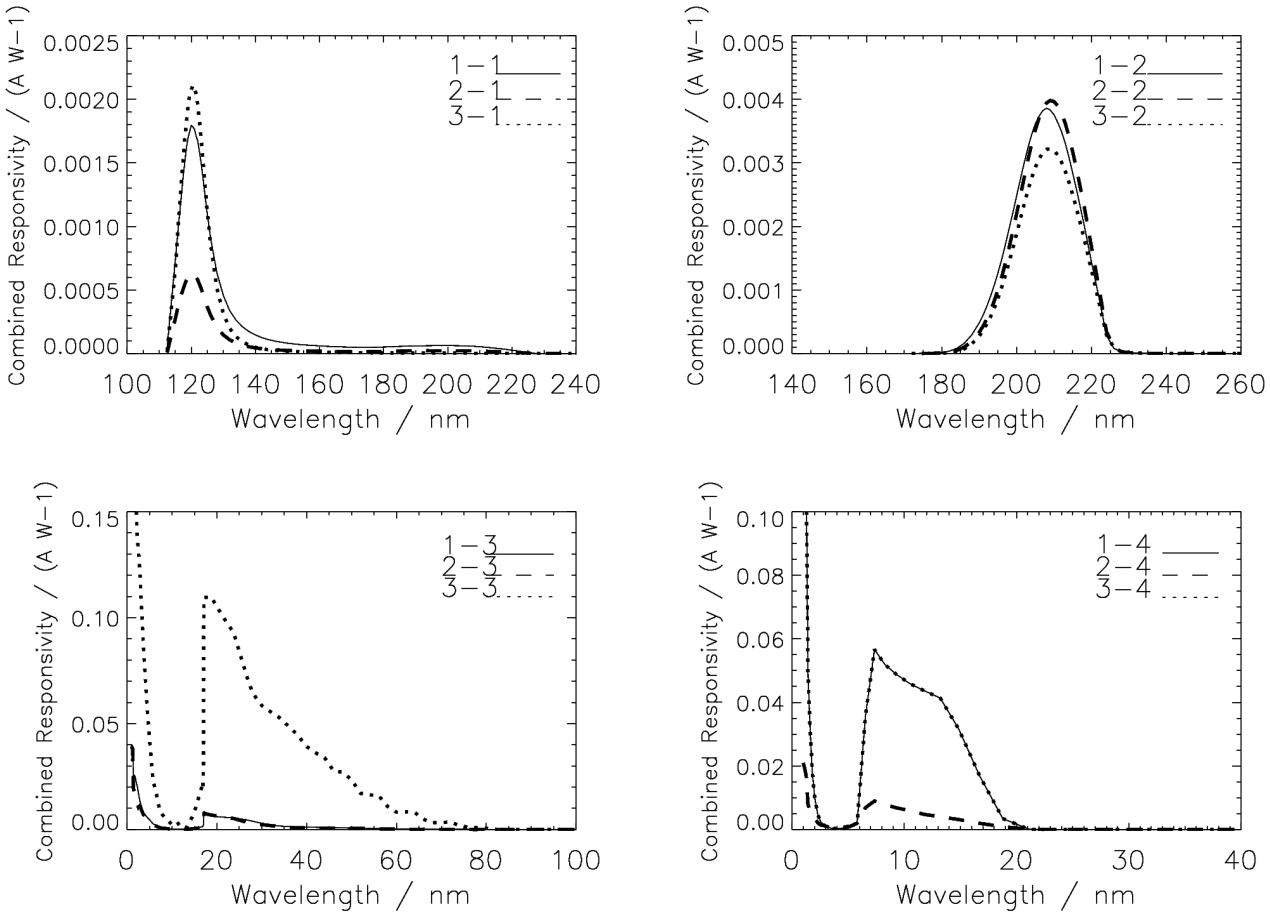

Figure 0. LYRA channel responsivities, similar to those presented at the Davos meeting, but updated with the latest responsivity measurements: Combination of filter and detector effects measured as a function of wavelength. *-1 = Lyman-alpha channels, *-2 = Herzberg channels, *-3 = Aluminium channels, *-4 = Zirconium channels.

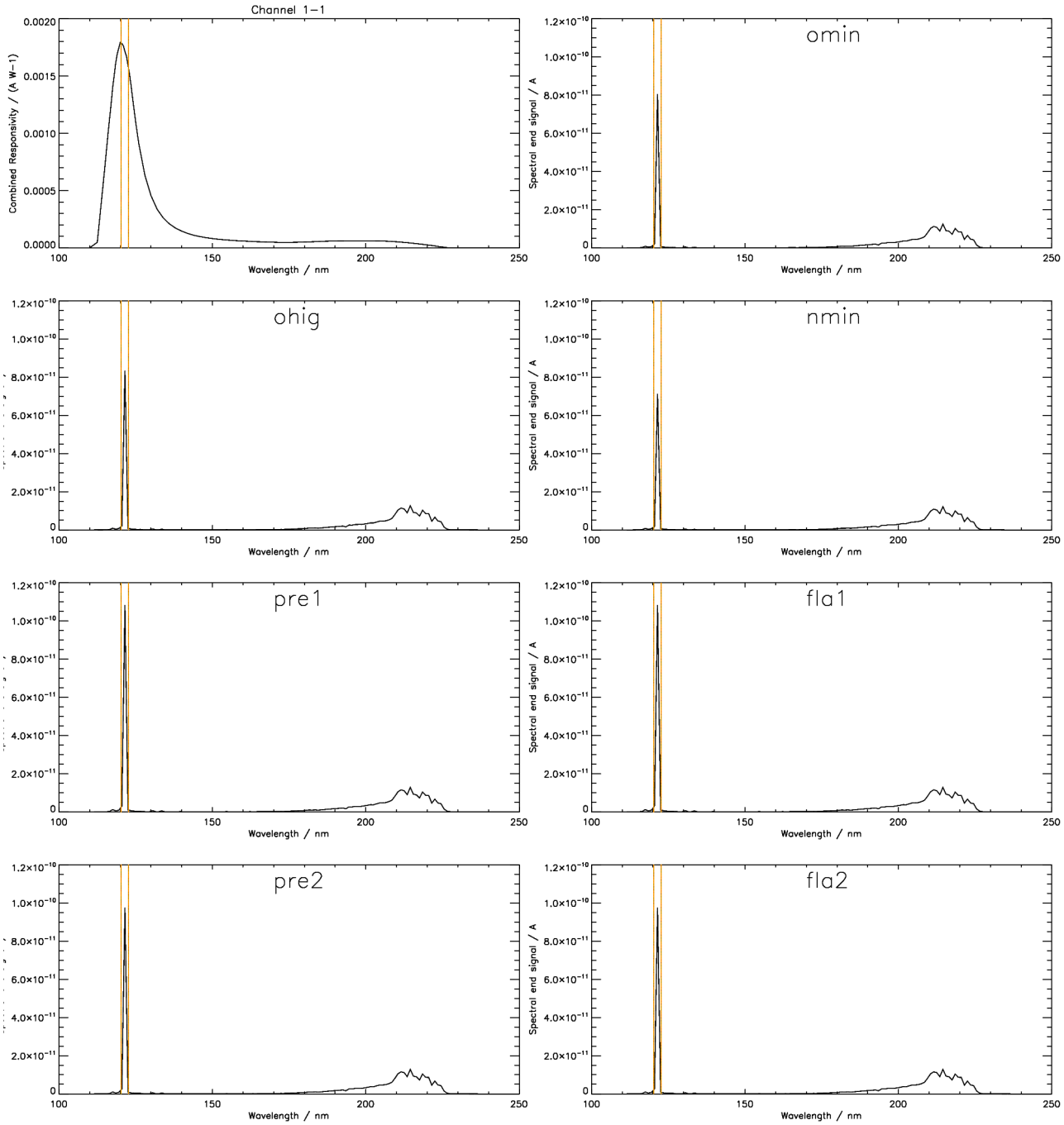

Figure 1-1. Measured responsivity and simulated output for LYRA channel 1-1
Ly XN + MSM12 (121.5 +/- nm)

sample	total	pure	residual	solar
omin	0.301267 nA	0.0831912 nA (27.6%)	0.218076 nA	0.00690130 Wm-2
ohig	0.308235 nA	0.0861396 nA (27.9%)	0.222095 nA	0.00714568 Wm-2
nmin	0.283186 nA	0.0735911 nA (26.0%)	0.209595 nA	0.00610500 Wm-2
pre1	0.339944 nA	0.112272 nA (33.0%)	0.227671 nA	0.00931232 Wm-2
fla1	0.339986 nA	0.112272 nA (33.0%)	0.227714 nA	0.00931232 Wm-2
pre2	0.327428 nA	0.100799 nA (30.8%)	0.226629 nA	0.00836111 Wm-2
fla2	0.327445 nA	0.100799 nA (30.8%)	0.226646 nA	0.00836111 Wm-2

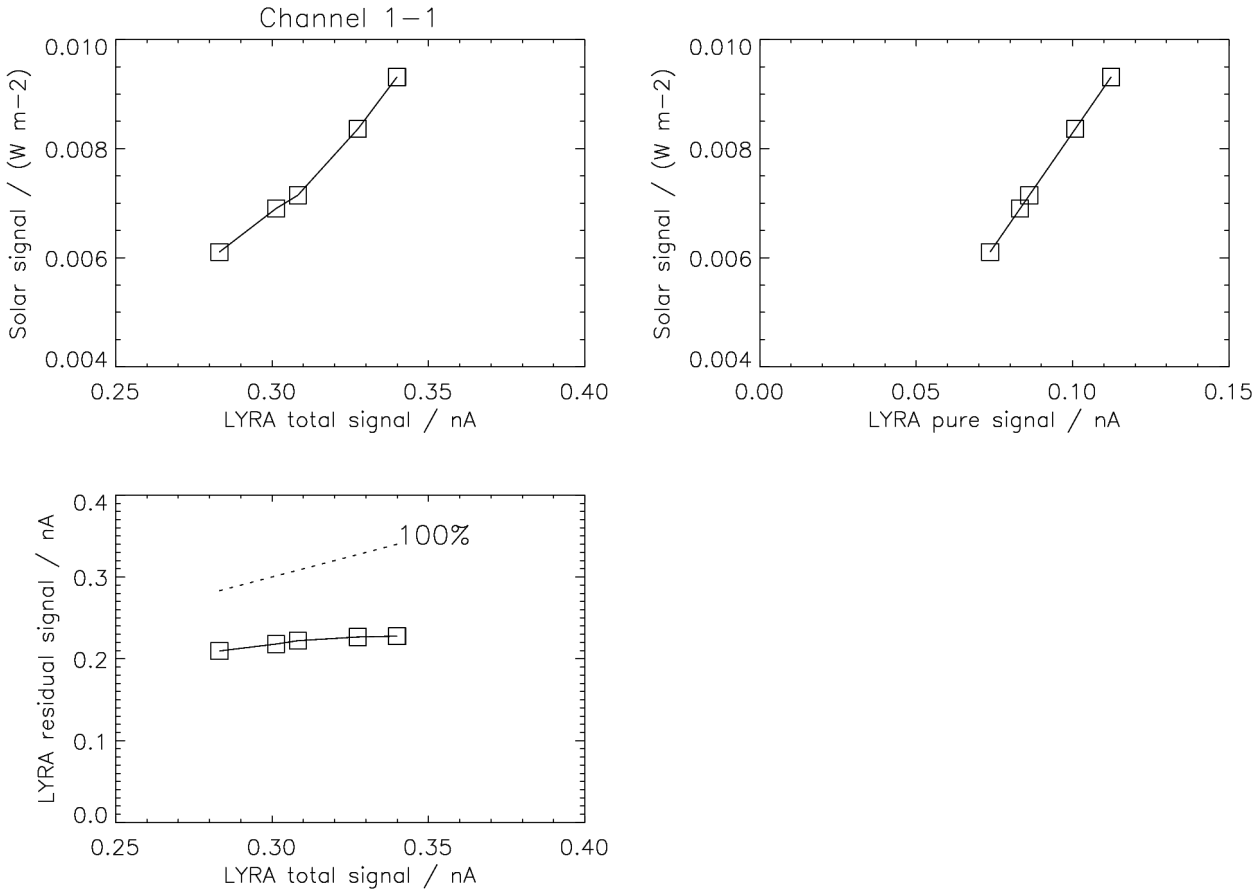

Figure 1-1a. Simulated relations between input and output for LYRA channel 1-1.

Remarks: Defining 2.5 nm around 121.5 nm as nominal interval leads to just three SORCE data points (120.5, 121.5, and 122.5 nm), of which only 121.5 nm is significant. This means that the simulation is essentially based on one value; a small variation of the nominal interval would not lead to different simulation results.

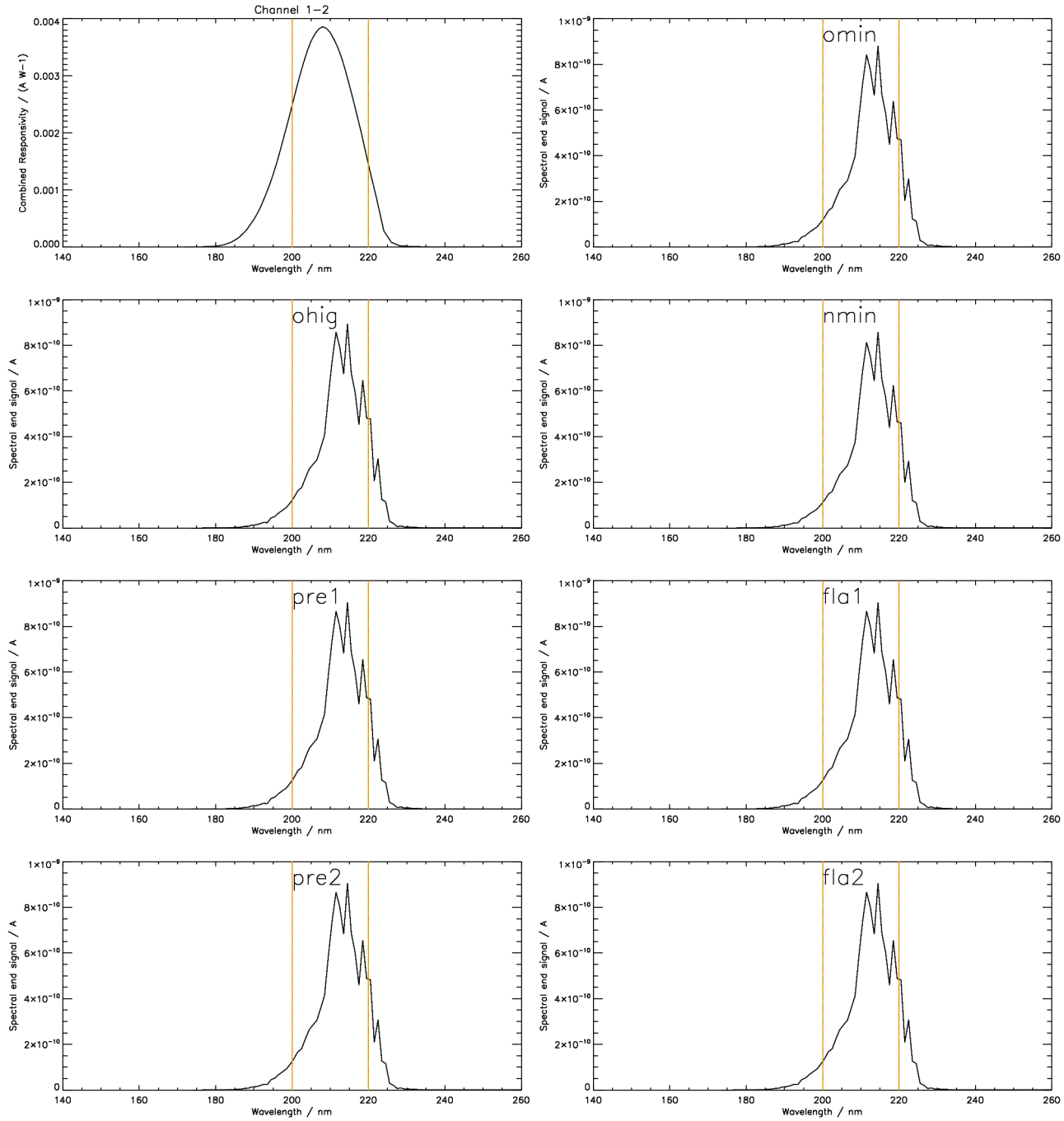

Figure 1-2. Measured responsivity and simulated output for LYRA channel 1-2
Herzberg + PIN10 (200-220 nm)

sample	total	pure	residual	solar
omin	11.3280 nA	9.49506 nA (83.8%)	1.83295 nA	0.461334 Wm-2
ohig	11.5311 nA	9.66663 nA (83.8%)	1.86449 nA	0.469345 Wm-2
nmin	10.9178 nA	9.14279 nA (83.7%)	1.77504 nA	0.445404 Wm-2
pre1	11.7096 nA	9.81582 nA (83.8%)	1.89378 nA	0.476369 Wm-2
fla1	11.7096 nA	9.81582 nA (83.8%)	1.89378 nA	0.476369 Wm-2
pre2	11.7057 nA	9.81157 nA (83.8%)	1.89416 nA	0.476294 Wm-2
fla2	11.7057 nA	9.81157 nA (83.8%)	1.89416 nA	0.476294 Wm-2

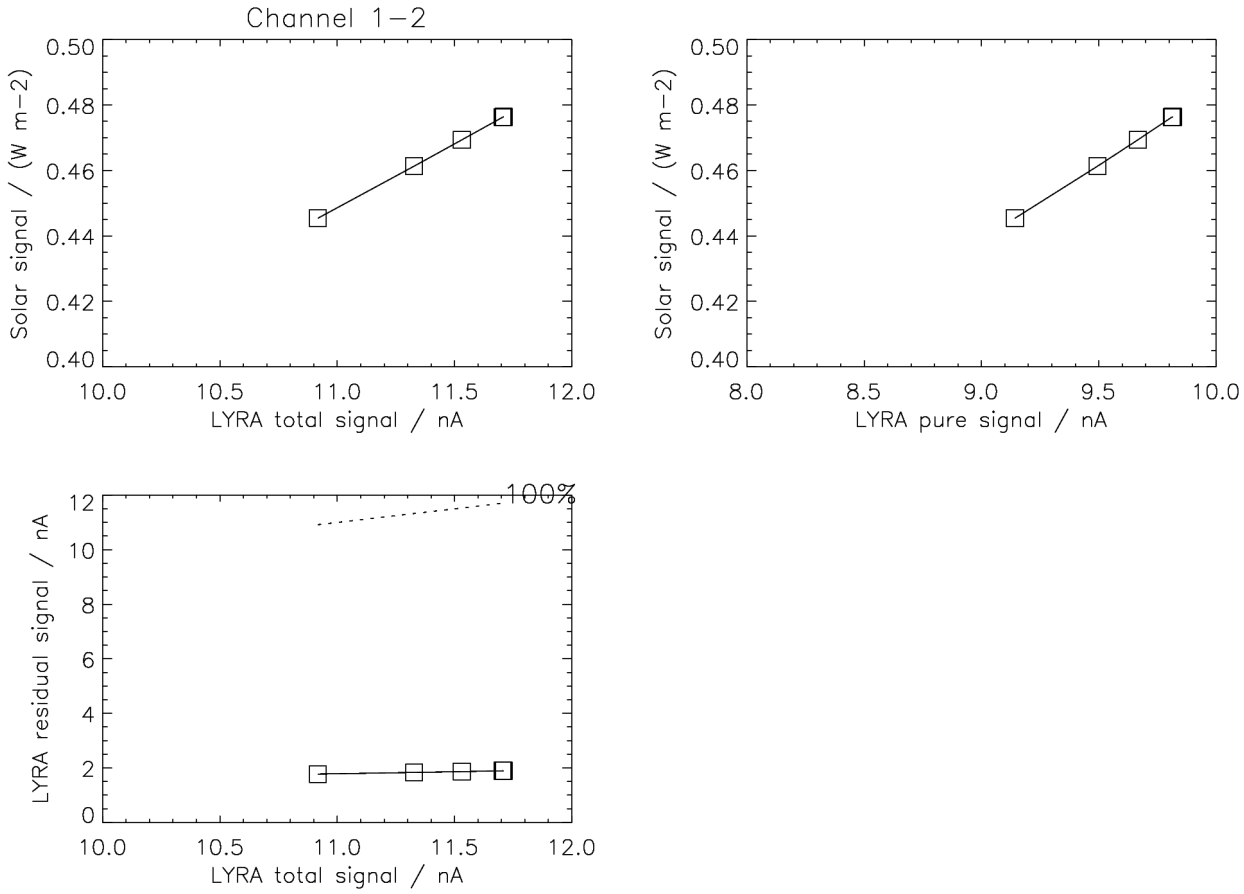

Figure 1-2a. Simulated relations between input and output for LYRA channel 1-2.

Remarks: The behavior of samples pre1, fla1, pre2, fla2 is approx. identical, thus there are only four significantly different data points. Please note the consequence for channel 1-1: While there is a different total and pure (Lyman-alpha) signal response for the last four samples, i.e. pre1,fla1 vs. pre2,fla2, the residual signal is approx. identical, because it is dominated by longer wavelengths - like the channel 1-2 signal shown here.

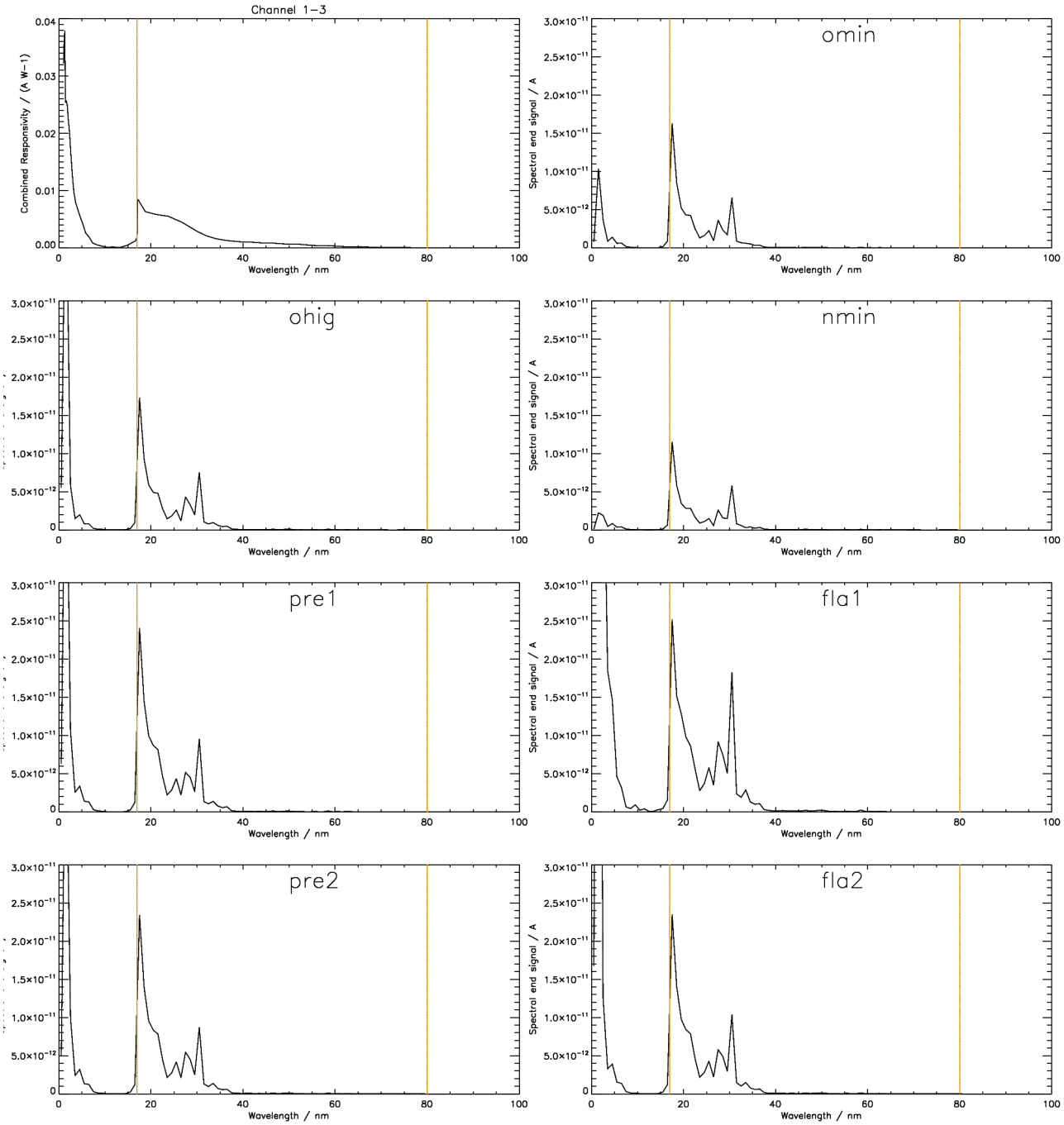

Figure 1-3. Measured responsivity and simulated output for LYRA channel 1-3
Aluminium + MSM11 (17-80 nm)

sample	total	pure	residual	solar
omin	0.0852873 nA	0.0656918 nA (77.0%)	0.0195955 nA	0.00225541 Wm-2
ohig	0.142513 nA	0.0745095 nA (52.3%)	0.0680032 nA	0.00263286 Wm-2
nmin	0.0541294 nA	0.0469544 nA (86.7%)	0.0071750 nA	0.00171904 Wm-2
pre1	0.196302 nA	0.110842 nA (56.5%)	0.0854606 nA	0.00376518 Wm-2
fla1	2.07897 nA	0.146527 nA (7.0%)	1.93244 nA	0.00570166 Wm-2
pre2	0.184207 nA	0.107000 nA (58.1%)	0.0772073 nA	0.00362499 Wm-2
fla2	0.291588 nA	0.111317 nA (38.2%)	0.180272 nA	0.00394254 Wm-2

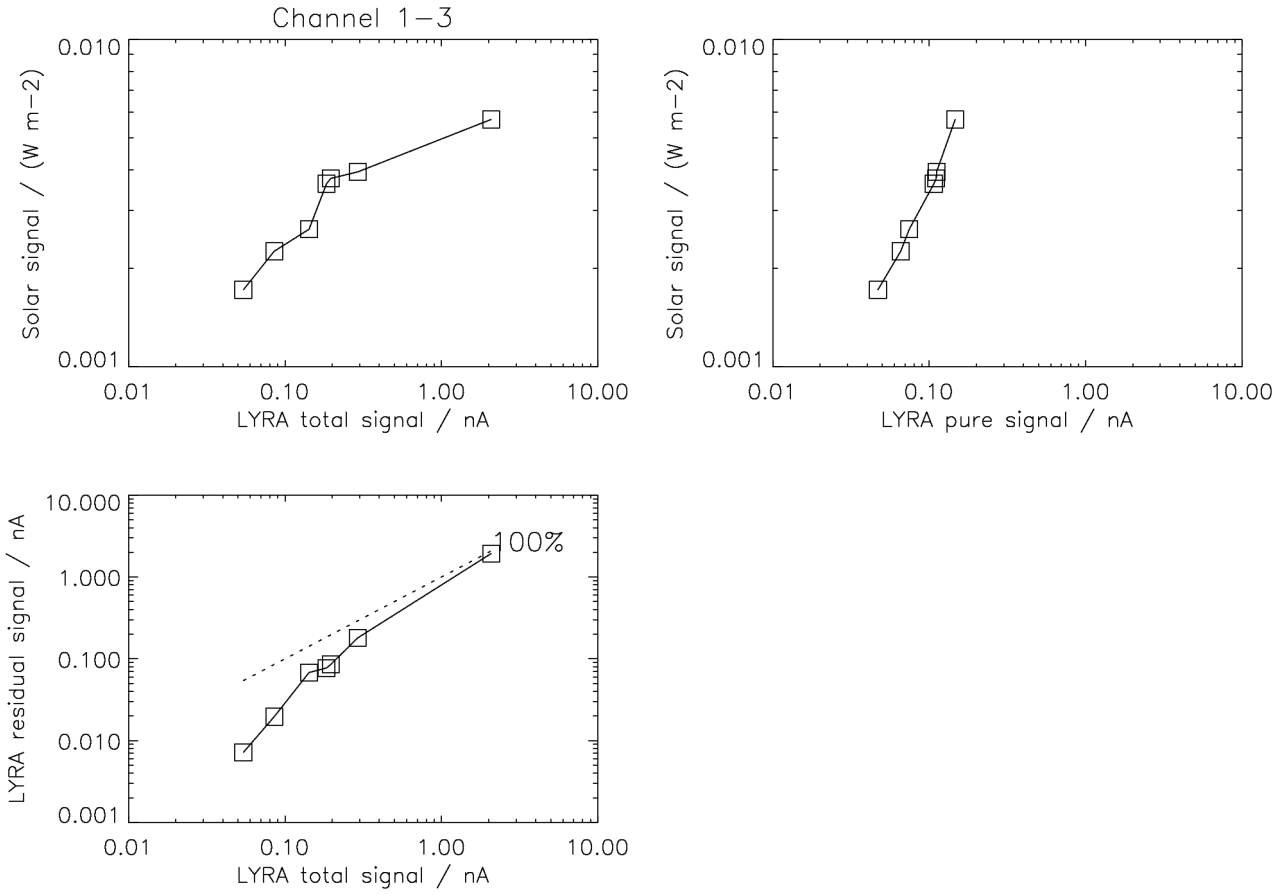

Figure 1-3a. Simulated relations between input and output for LYRA channel 1-3.

Remarks: The functional relation between the solar signal and the LYRA total signal is still not quite straightforward (but much less irregular than before the "new-spectra" update, compare upper left image before and after). The reason for nonlinearity is a contamination due to the influence of the interval below ~10 nm, which is not part of the 17-80 nm nominal interval of the Al channels. - Although the channel interval nominally reaches up to 80 nm, effectively it appears to end at 35 nm (see Figure 1-3). - For the small subset of flare events, the uncalibrated data of this channel (i.e. before subtraction of the substantial short-wavelength contamination) will probably not be very meaningful.

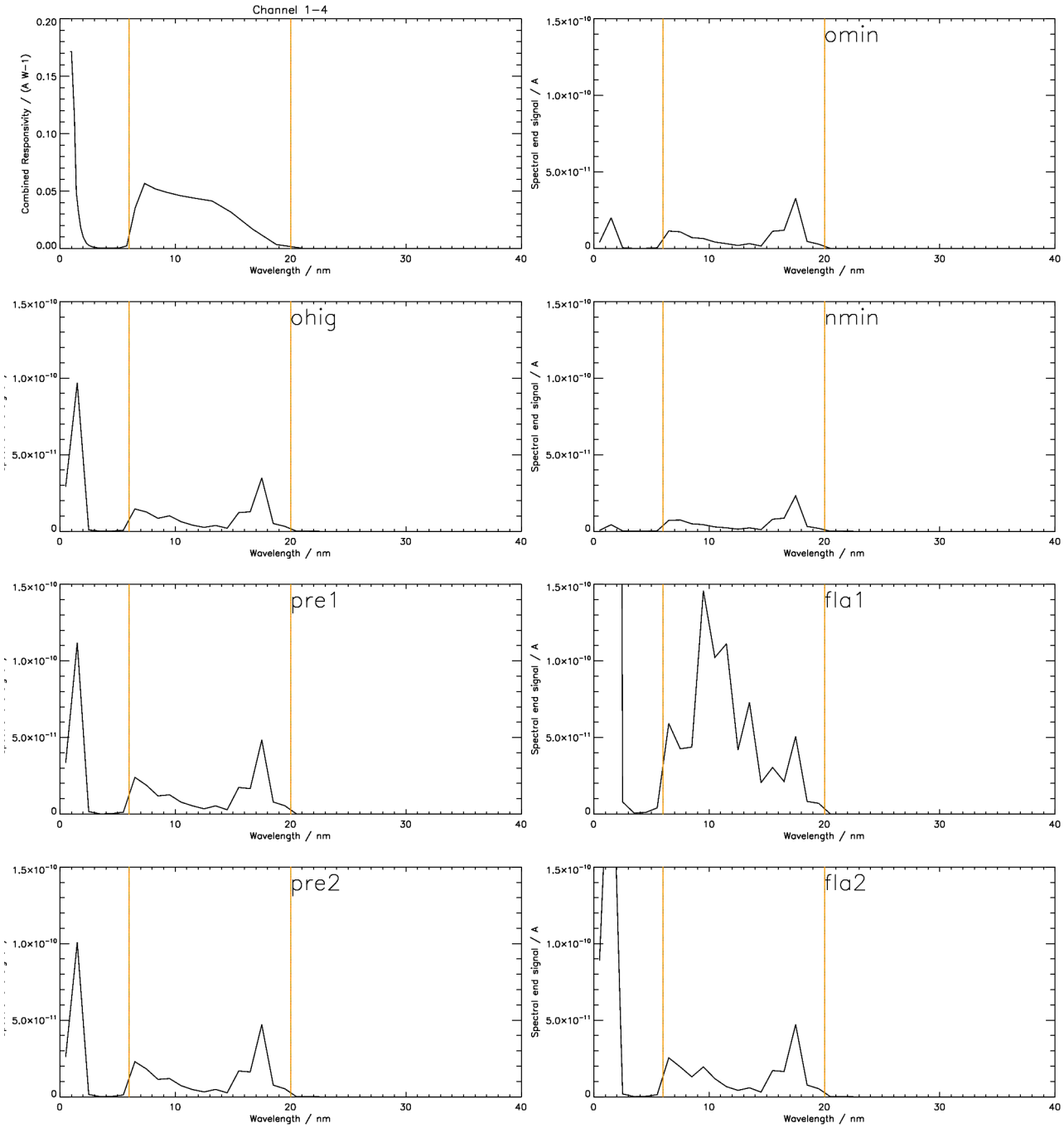

Figure 1-4. Measured responsivity and simulated output for LYRA channel 1-4
Zr(300nm) + AXUV20D (6-20 nm)

sample	total	pure	residual	solar
omin	0.140574 nA	0.113323 nA (80.6%)	0.0272501 nA	0.000889638 Wm-2
ohig	0.261593 nA	0.131955 nA (50.4%)	0.129639 nA	0.000996023 Wm-2
nmin	0.085286 nA	0.077910 nA (91.4%)	0.00737640 nA	0.000612958 Wm-2
pre1	0.337455 nA	0.187175 nA (55.5%)	0.150281 nA	0.00146242 Wm-2
fla1	5.37328 nA	0.757063 nA (14.1%)	4.61622 nA	0.00340528 Wm-2
pre2	0.311291 nA	0.179567 nA (57.7%)	0.131724 nA	0.00141076 Wm-2
fla2	0.565202 nA	0.202588 nA (35.8%)	0.362615 nA	0.00148986 Wm-2

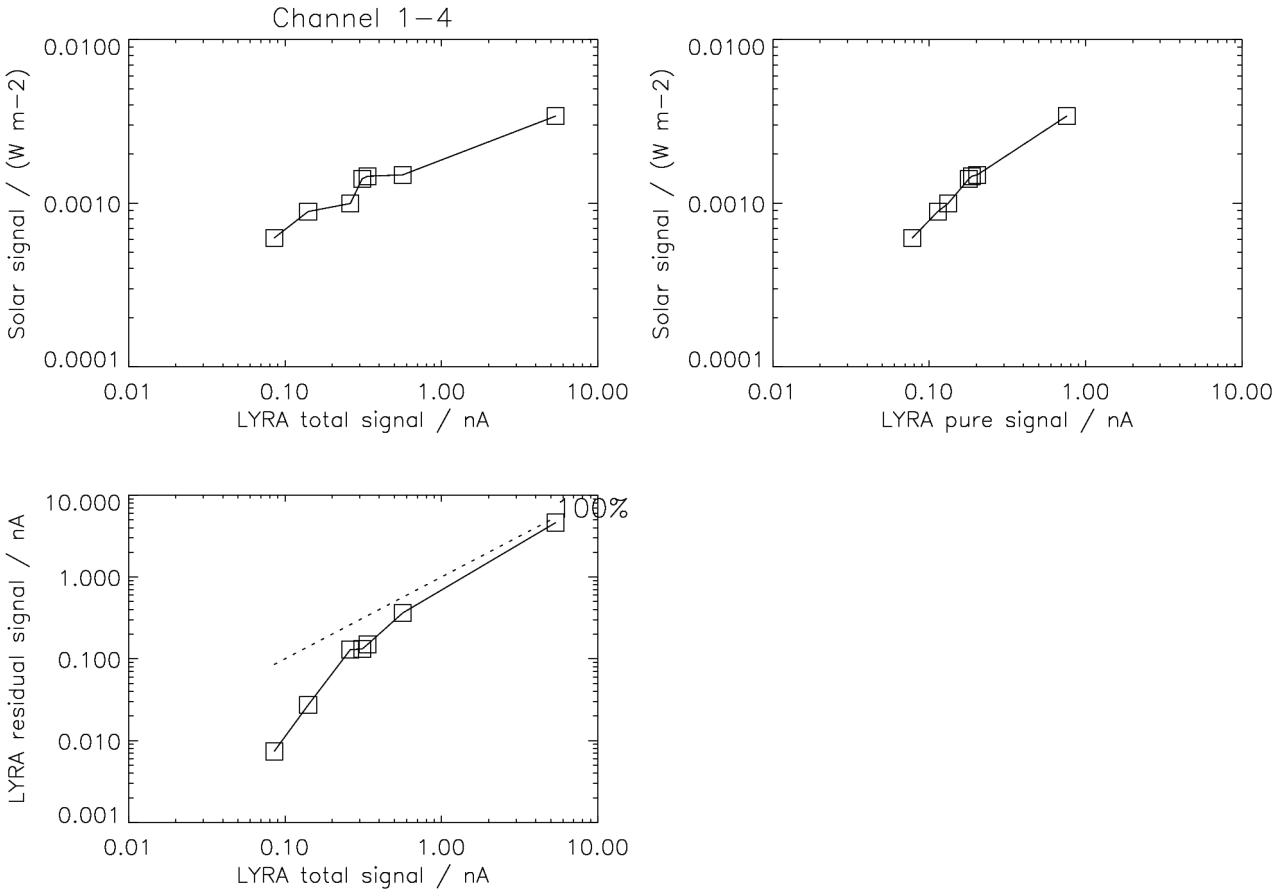

Figure 1-4a. Simulated relations between input and output for LYRA channel 1-4.

Remarks: After redefining the nominal interval of the Zr channel, the functional relation between the solar signal and the LYRA total signal is not straightforward any more, but rather resembles the Al channel. The reason for nonlinearity is a contamination due to the influence of the interval below ~3 nm, which is not part of the new 6-20 nm nominal interval of the Zr channels. - For the small subset of flare events, the uncalibrated data of this channel (i.e. before subtraction of the substantial short-wavelength contamination) will probably not be very meaningful.

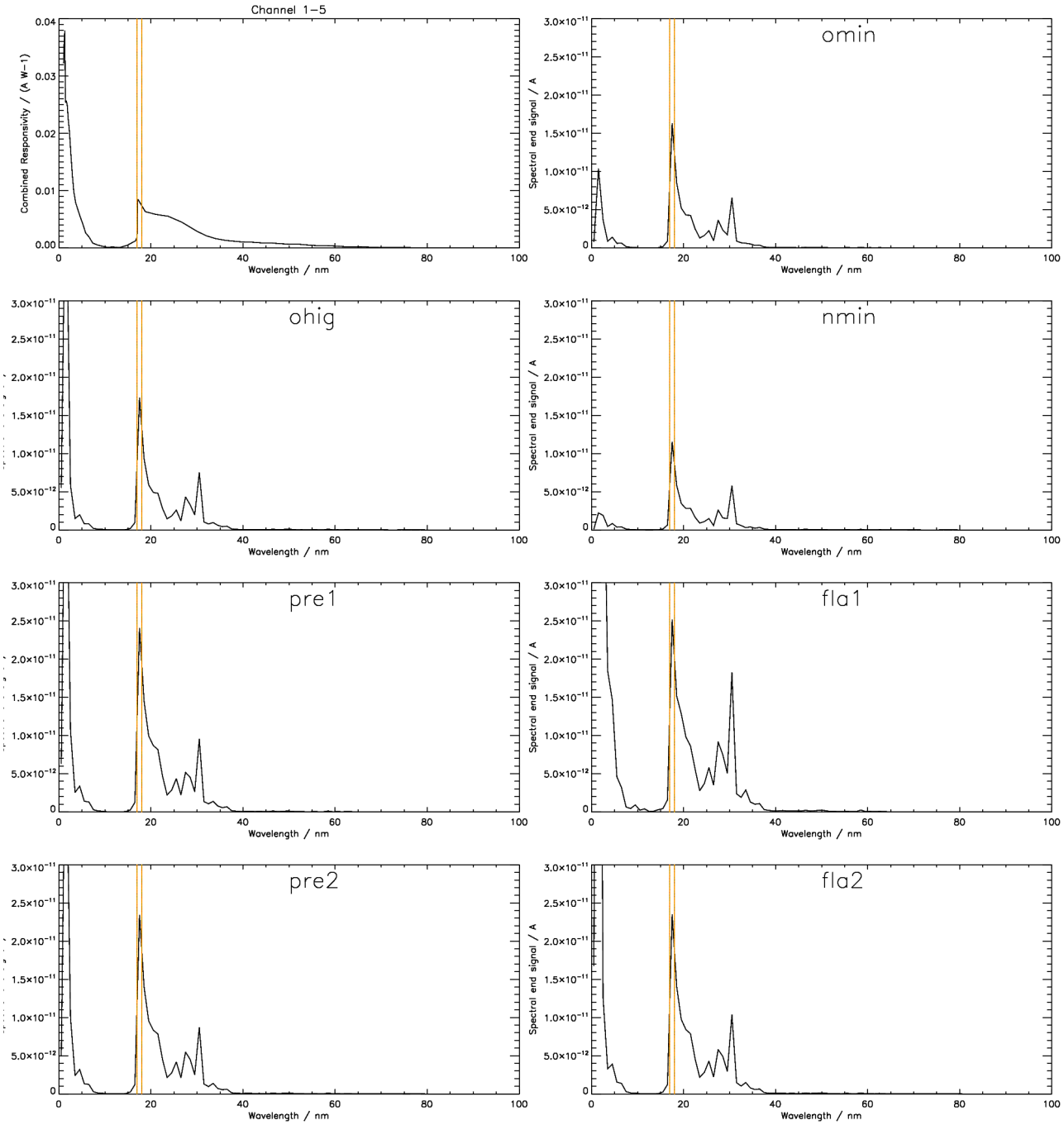

Figure 1-5. Measured responsivity and simulated output for the *virtual* LYRA channel 1-5 Aluminium + MSM11 *(17-18 nm, for cross-calibration with SWAP)*

sample	total	pure	residual	solar
omin	0.0852873 nA	0.0162957 nA (19.1%)	0.0689916 nA	0.000274049 Wm-2
ohig	0.142513 nA	0.0173253 nA (12.2%)	0.125187 nA	0.000291364 Wm-2
nmin	0.0541294 nA	0.0115330 nA (21.3%)	0.0425964 nA	0.000193953 Wm-2
pre1	0.196302 nA	0.0240601 nA (12.3%)	0.172242 nA	0.000404624 Wm-2
fla1	2.07897 nA	0.0251771 nA (1.2%)	2.05379 nA	0.000423409 Wm-2
pre2	0.184207 nA	0.0234346 nA (12.7%)	0.160772 nA	0.000394106 Wm-2
fla2	0.291588 nA	0.0234881 nA (8.1%)	0.268100 nA	0.000395006 Wm-2

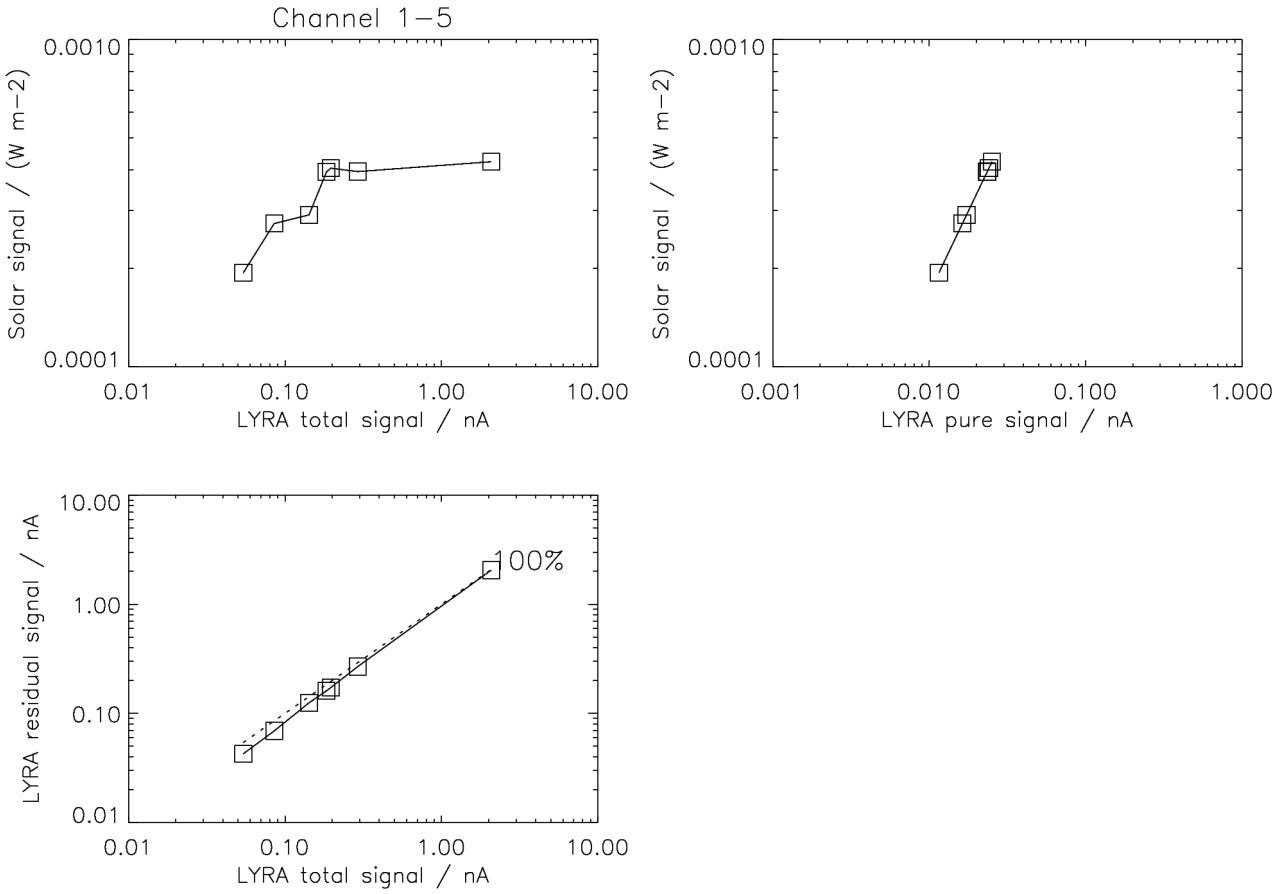

Figure 1-5a. Simulated relations between input and output for *virtual* LYRA channel 1-5.

Remarks: The functional relation between the (SWAP) solar signal and the LYRA total signal is not straightforward. One reason for nonlinearity is a contamination due to the influence of the interval below ~10 nm. It appears that a flare will hardly influence the solar irradiance as measured by SWAP.

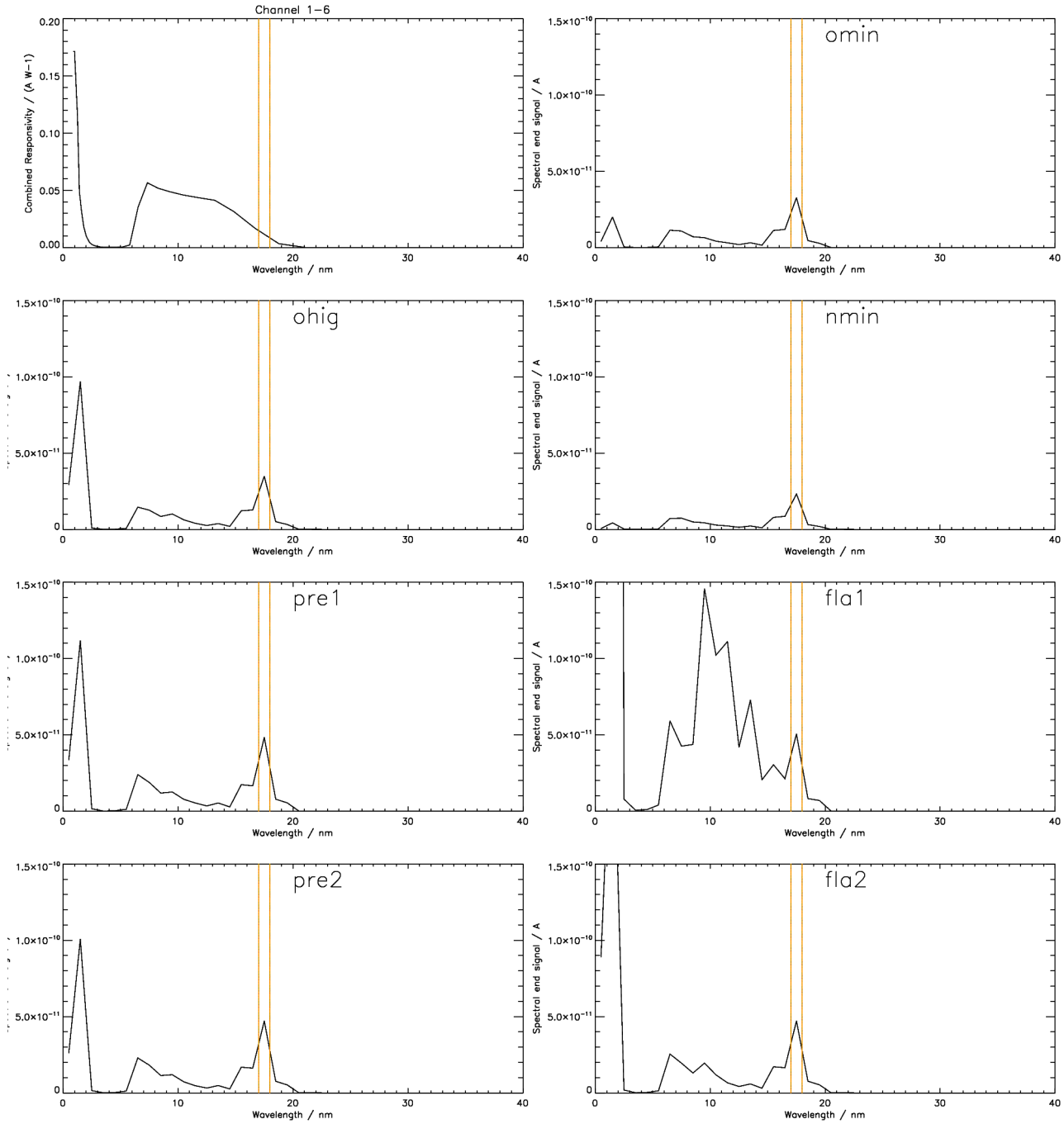

Figure 1-6. Measured responsivity and simulated output for the *virtual* LYRA channel 1-6 Zr(300nm) + AXUV20D *(17-18 nm, for cross-calibration with SWAP)*

sample	total	pure	residual	solar
omin	0.140574 nA	0.0327458 nA (23.3%)	0.107828 nA	0.000274049 Wm-2
ohig	0.261593 nA	0.0348147 nA (13.3%)	0.226779 nA	0.000291364 Wm-2
nmin	0.0852863 nA	0.0231752 nA (27.2%)	0.0621111 nA	0.000193953 Wm-2
pre1	0.337455 nA	0.0483480 nA (14.3%)	0.289107 nA	0.000404624 Wm-2
fla1	5.37328 nA	0.0505926 nA (0.9%)	5.32269 nA	0.000423409 Wm-2
pre2	0.311291 nA	0.0470912 nA (15.1%)	0.264199 nA	0.000394106 Wm-2
fla2	0.565202 nA	0.0471988 nA (8.4%)	0.518004 nA	0.000395006 Wm-2

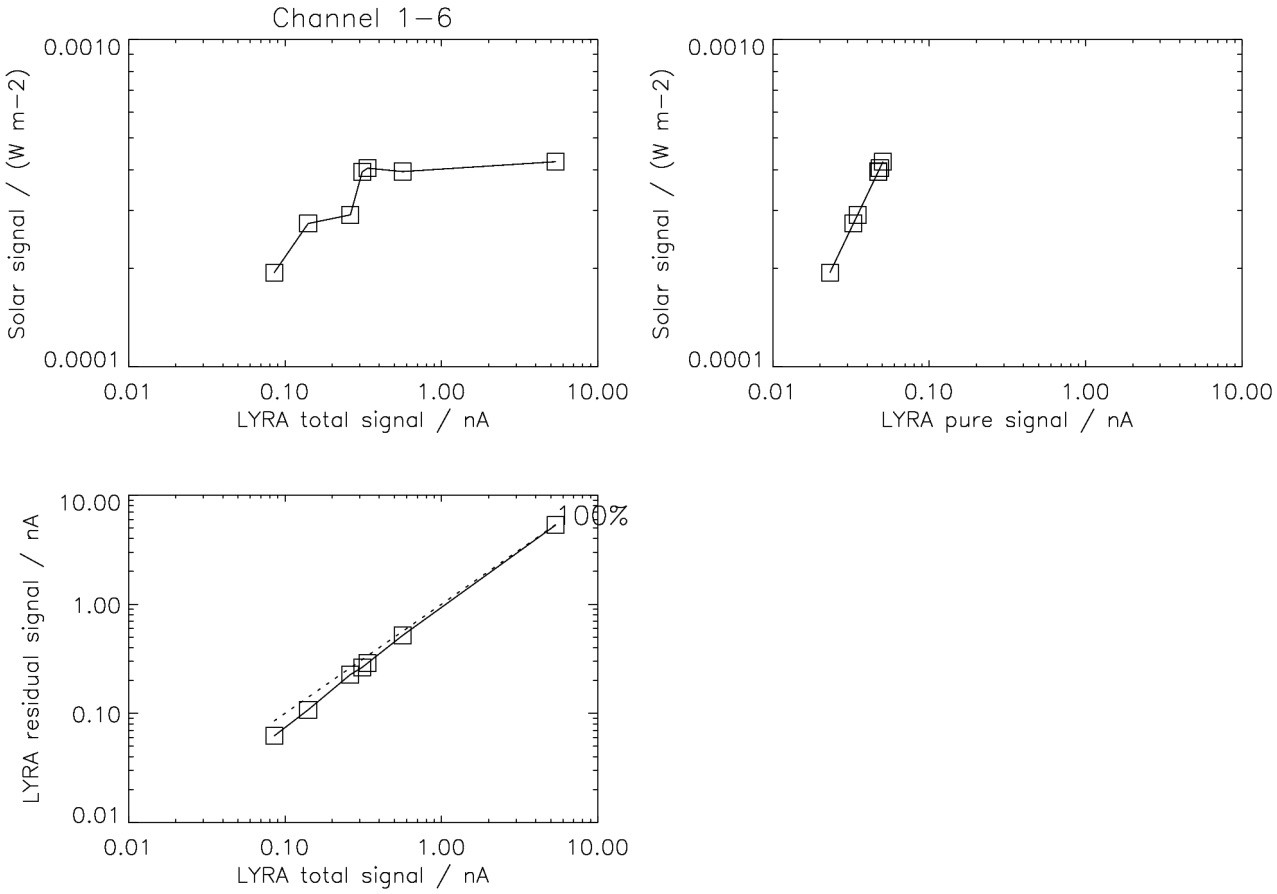

Figure 1-6a. Simulated relations between input and output for *virtual* LYRA channel 1-6.

Remarks: The functional relation between the (SWAP) solar signal and the LYRA total signal is not straightforward. One reason for nonlinearity is a contamination due to the influence of the interval below ~3 nm. It appears that a flare will hardly influence the solar irradiance as measured by SWAP.

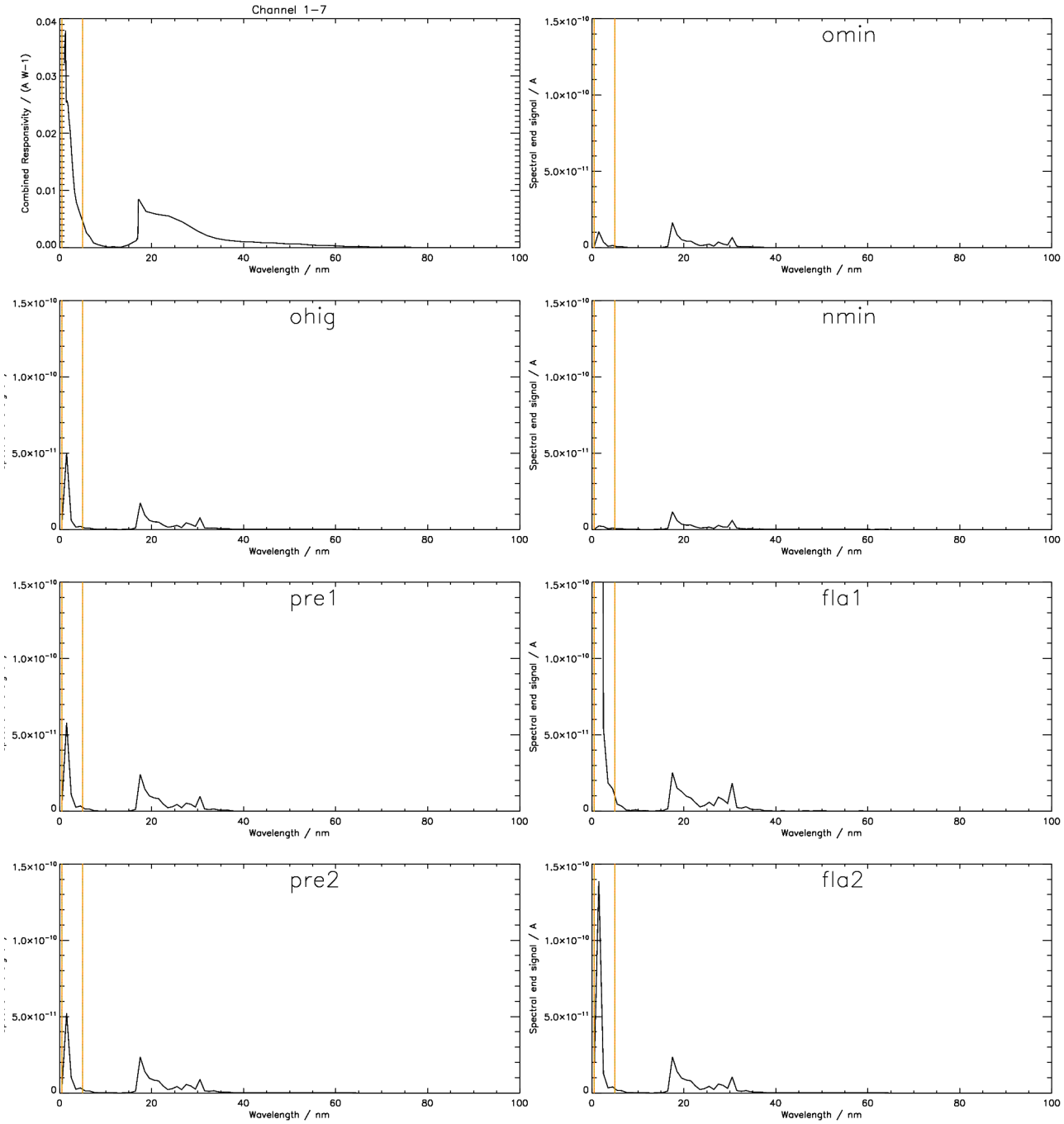

Figure 1-7. Measured responsivity and simulated output for the *virtual* LYRA channel 1-7
Aluminium + MSM11 *(< 5 nm, for cross-calibration with TIMED/SEE, or additional product?)*

sample	total	pure	residual	solar
omin	0.0852873 nA	0.0170338 nA (20.0%)	0.0682535 nA	0.000143220 Wm-2
ohig	0.142513 nA	0.0649144 nA (45.5%)	0.0775984 nA	0.000430065 Wm-2
nmin	0.0541294 nA	0.0054809 nA (10.1%)	0.0486485 nA	0.0000581368 Wm-2
pre1	0.196302 nA	0.0807515 nA (41.1%)	0.115551 nA	0.000572517 Wm-2
fla1	2.07897 nA	1.91968 nA (92.3%)	0.159291 nA	0.0109987 Wm-2
pre2	0.184207 nA	0.0726816 nA (39.5%)	0.111525 nA	0.000521914 Wm-2
fla2	0.291588 nA	0.175256 nA (60.1%)	0.116332 nA	0.00111161 Wm-2

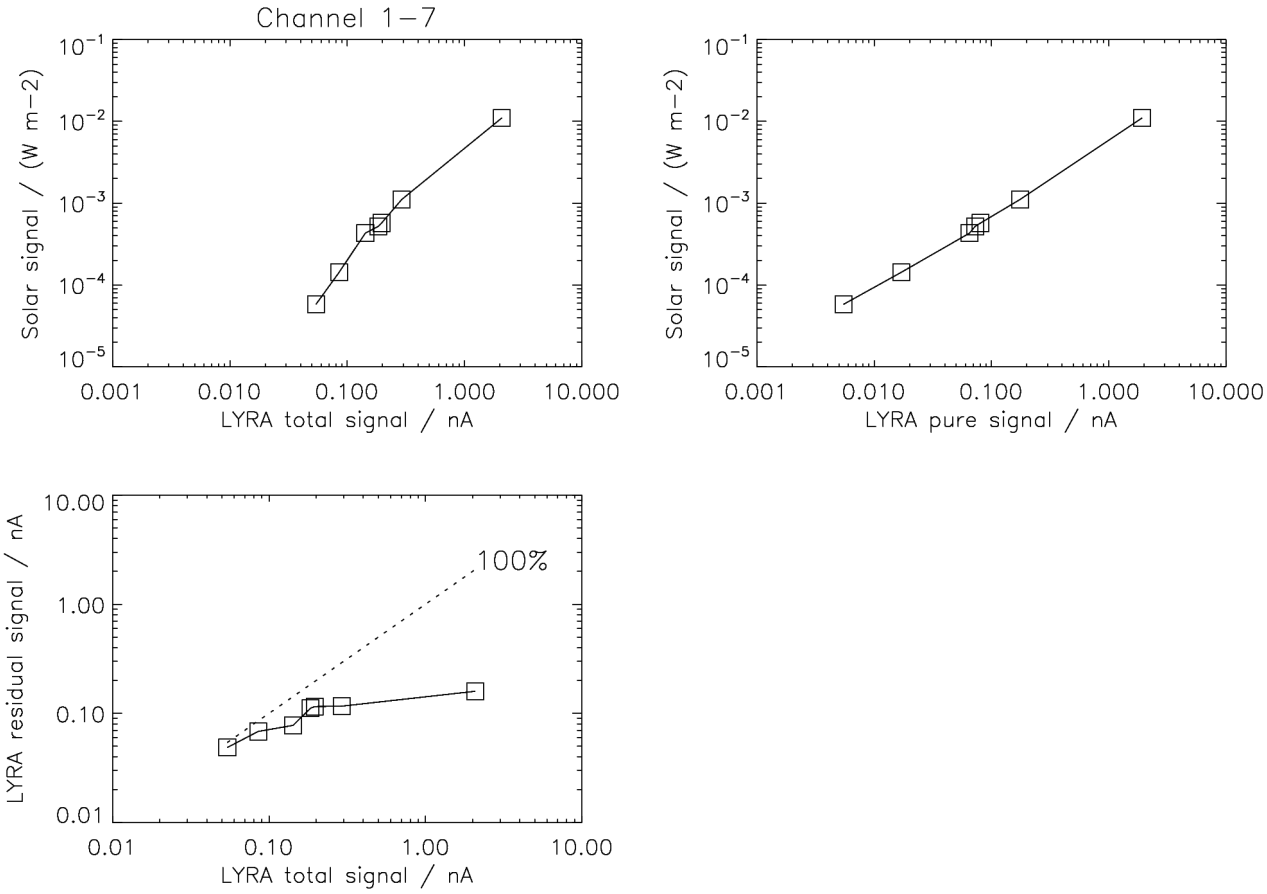

Figure 1-7a. Simulated relations between input and output for *virtual* LYRA channel 1-7.

Remarks: The functional relation between the (< 5 nm, SXR) solar signal and the LYRA total signal is not straightforward, because (a) the channel's responsivity is higher for short wavelengths, and (b) the EUV signal dominates in non-flare situations.

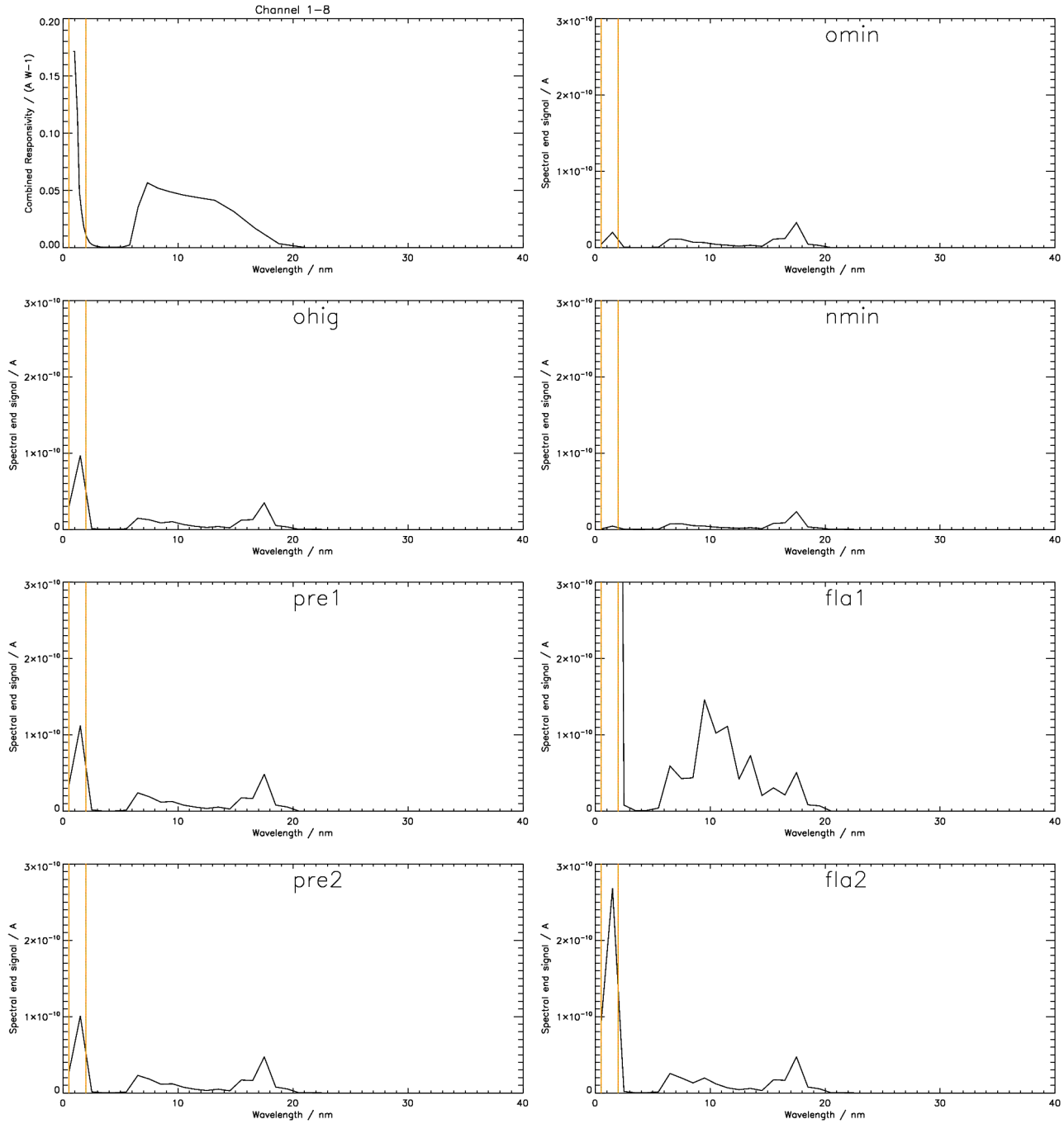

Figure 1-8. Measured responsivity and simulated output for the *virtual* LYRA channel 1-8
Zr(300nm) + AXUV20D *(< 2 nm, for cross-calibration with TIMED/SEE, or additional product?)*

sample	total	pure	residual	solar
omin	0.140574 nA	0.0241494 nA (17.2%)	0.116424 nA	0.0000611985 Wm-2
ohig	0.261593 nA	0.125961 nA (48.2%)	0.135632 nA	0.000303303 Wm-2
nmin	0.085286 nA	0.0048156 nA (5.6%)	0.0804707 nA	0.0000127735 Wm-2
pre1	0.337455 nA	0.145184 nA (43.0%)	0.192271 nA	0.000350038 Wm-2
fla1	5.37328 nA	4.60069 nA (85.6%)	0.772594 nA	0.00983327 Wm-2
pre2	0.311291 nA	0.126798 nA (40.7%)	0.184492 nA	0.000312139 Wm-2
fla2	0.565202 nA	0.357056 nA (63.2%)	0.208146 nA	0.000846606 Wm-2

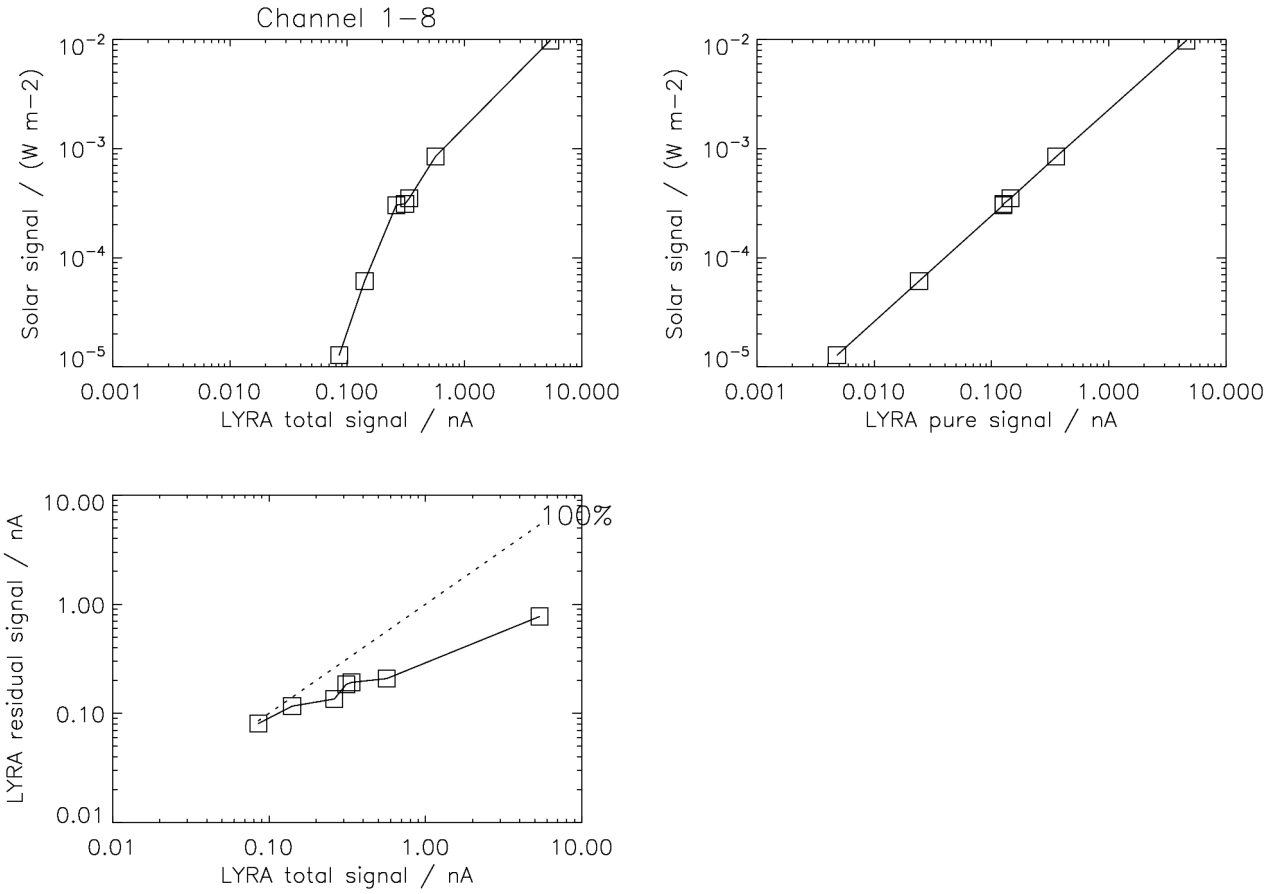

Figure 1-8a. Simulated relations between input and output for *virtual* LYRA channel 1-8.

Remarks: The functional relation between the (< 2 nm, SXR) solar signal and the LYRA total signal is not straightforward, because (a) the channel's responsivity is higher for short wavelengths, and (b) the EUV signal dominates in non-flare situations.

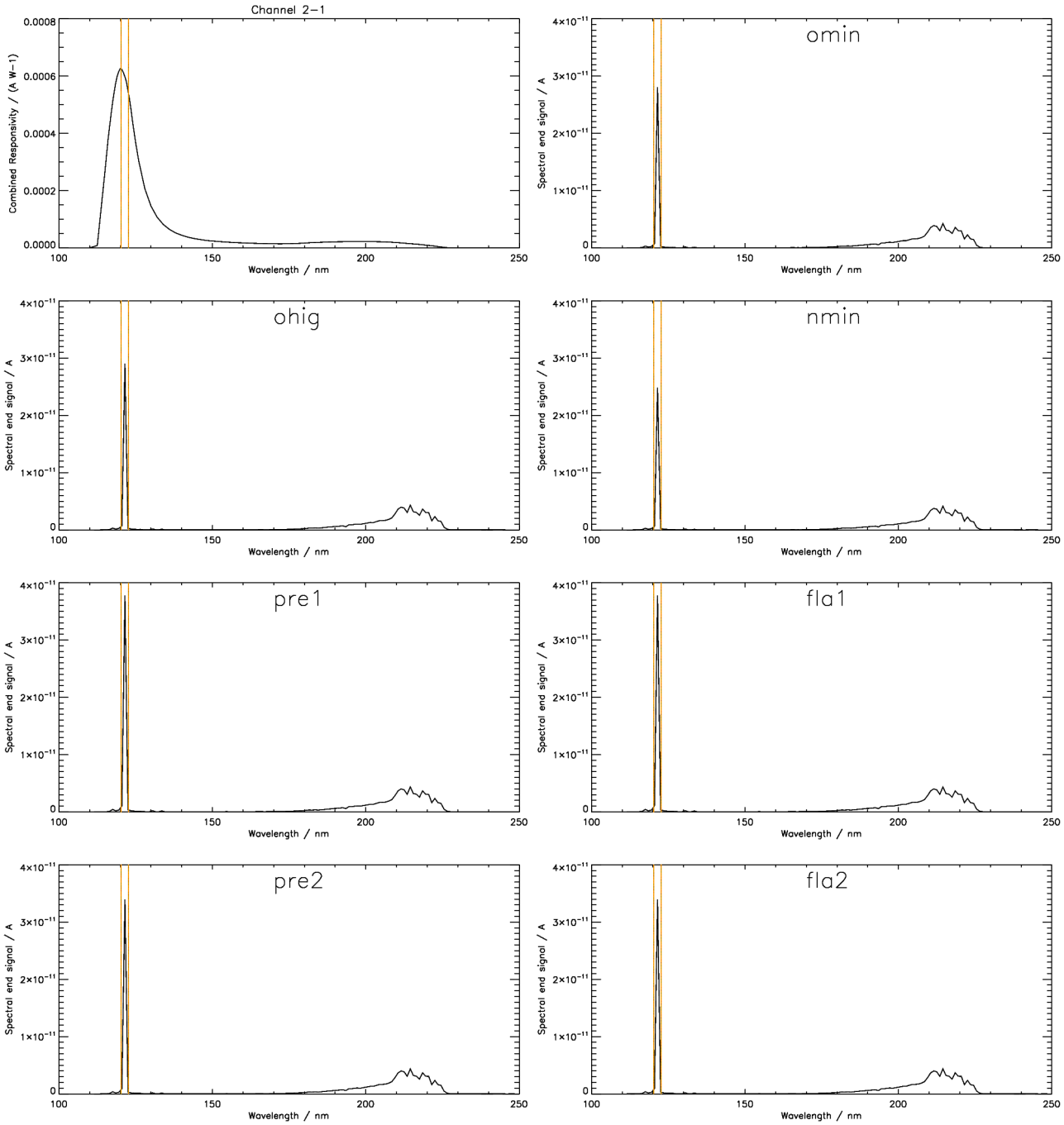

Figure 2-1. Measured responsivity and simulated output for LYRA channel 2-1
Ly XN + MSM21 (121.5 +/- nm)

sample	total	pure	residual	solar
omin	0.105905 nA	0.0289875 nA (27.4%)	0.0769172 nA	0.00690130 Wm-2
ohig	0.108327 nA	0.0300149 nA (27.7%)	0.0783118 nA	0.00714568 Wm-2
nmin	0.099602 nA	0.0256423 nA (25.7%)	0.0739601 nA	0.00610500 Wm-2
pre1	0.119349 nA	0.0391210 nA (32.8%)	0.0802279 nA	0.00931232 Wm-2
fla1	0.119359 nA	0.0391210 nA (32.8%)	0.0802381 nA	0.00931232 Wm-2
pre2	0.115001 nA	0.0351230 nA (30.5%)	0.0798784 nA	0.00836111 Wm-2
fla2	0.115004 nA	0.0351230 nA (30.5%)	0.0798813 nA	0.00836111 Wm-2

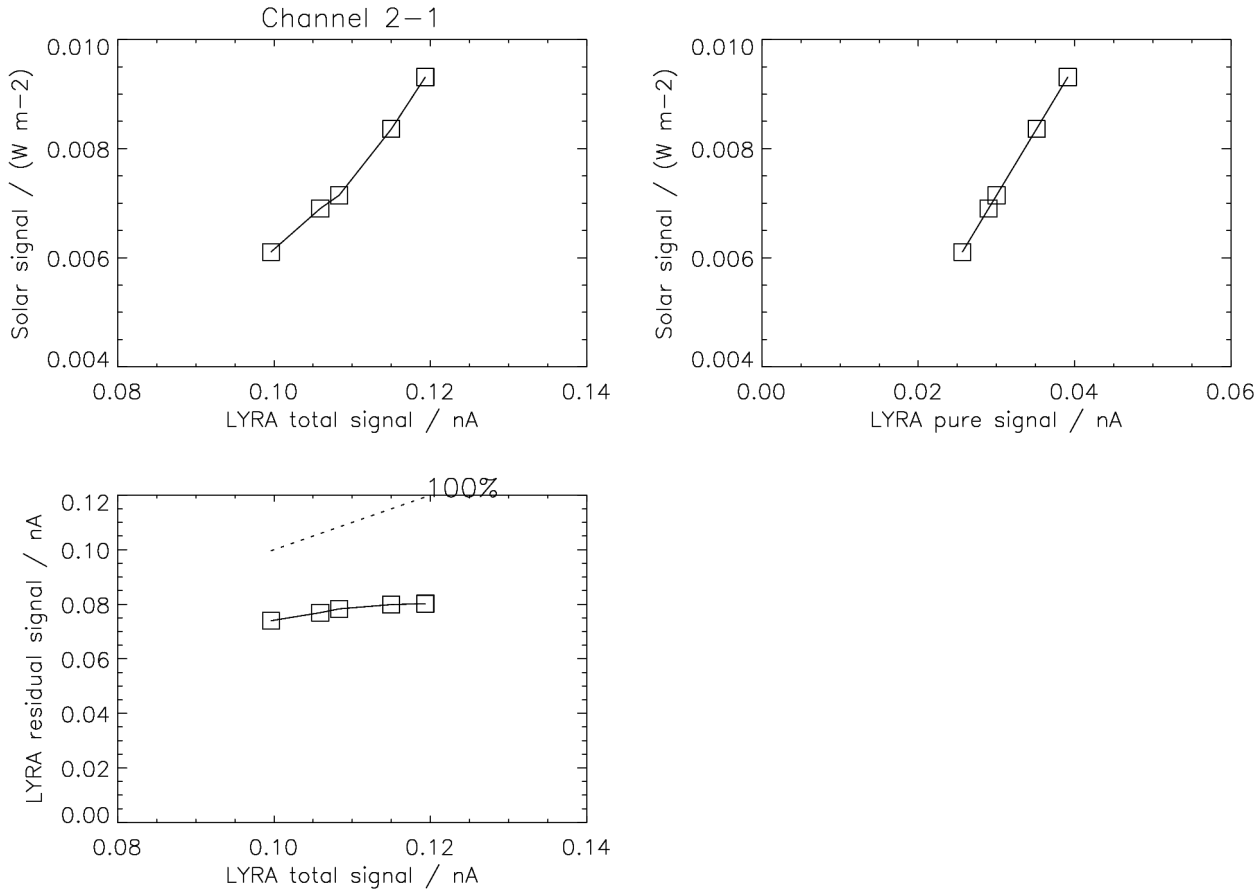

Figure 2-1a. Simulated relations between input and output for LYRA channel 2-1.

Remarks: Defining 2.5 nm around 121.5 nm as nominal interval leads to just three SORCE data points (120.5, 121.5, and 122.5 nm), of which only 121.5 nm is significant. This means that the simulation is essentially based on one value; a small variation of the nominal interval would not lead to different simulation results.

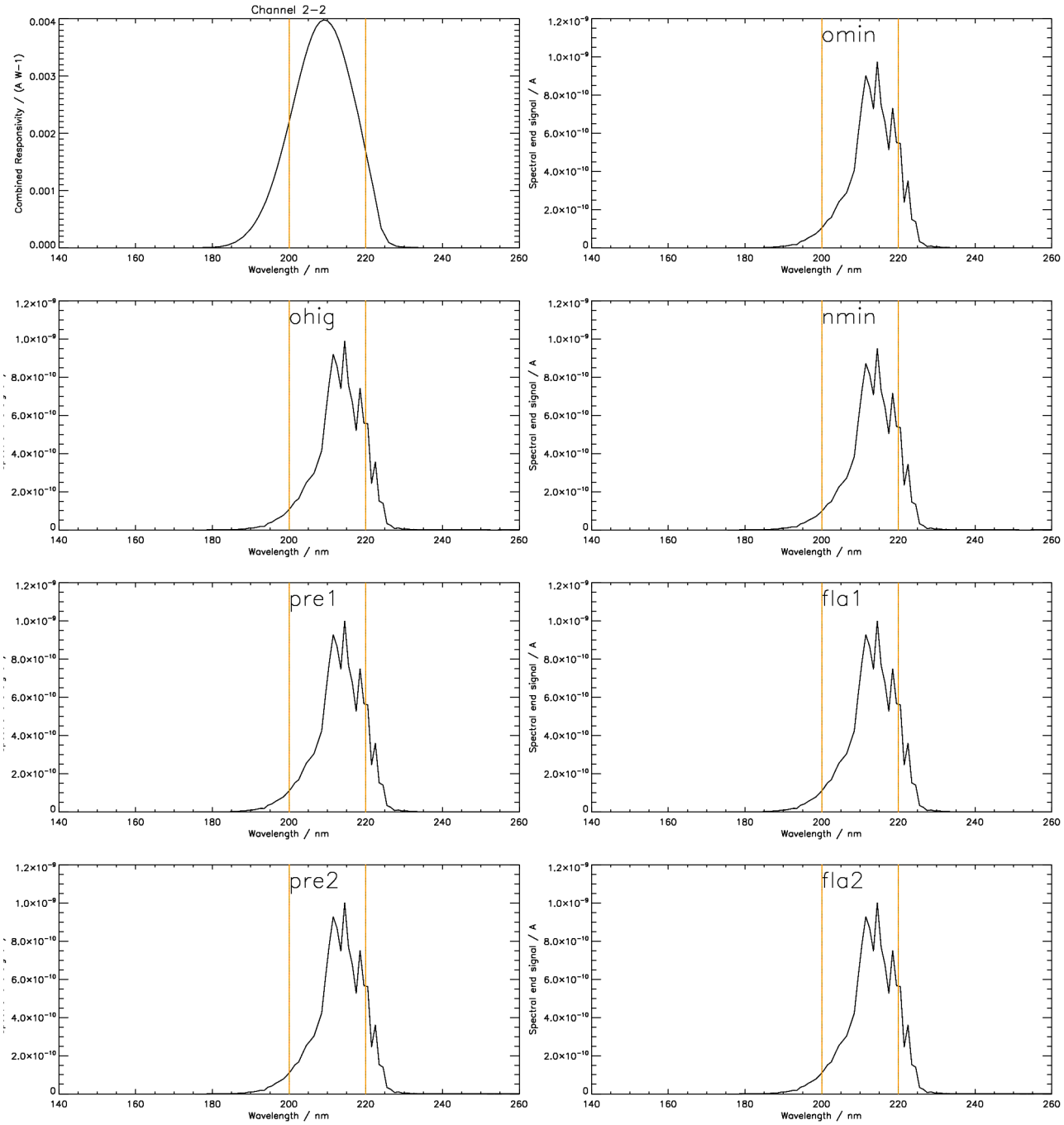

Figure 2-2. Measured responsivity and simulated output for LYRA channel 2-2
Herzberg + PIN11 (200-220 nm)

sample	total	pure	residual	solar
omin	12.1142 nA	10.1644 nA (83.9%)	1.94981 nA	0.461334 Wm-2
ohig	12.3278 nA	10.3455 nA (83.9%)	1.98233 nA	0.469345 Wm-2
nmin	11.6904 nA	9.7972 nA (83.8%)	1.89315 nA	0.445404 Wm-2
pre1	12.5120 nA	10.5015 nA (83.9%)	2.01056 nA	0.476369 Wm-2
fla1	12.5120 nA	10.5015 nA (83.9%)	2.01056 nA	0.476369 Wm-2
pre2	12.5103 nA	10.4984 nA (83.9%)	2.01191 nA	0.476294 Wm-2
fla2	12.5103 nA	10.4984 nA (83.9%)	2.01191 nA	0.476294 Wm-2

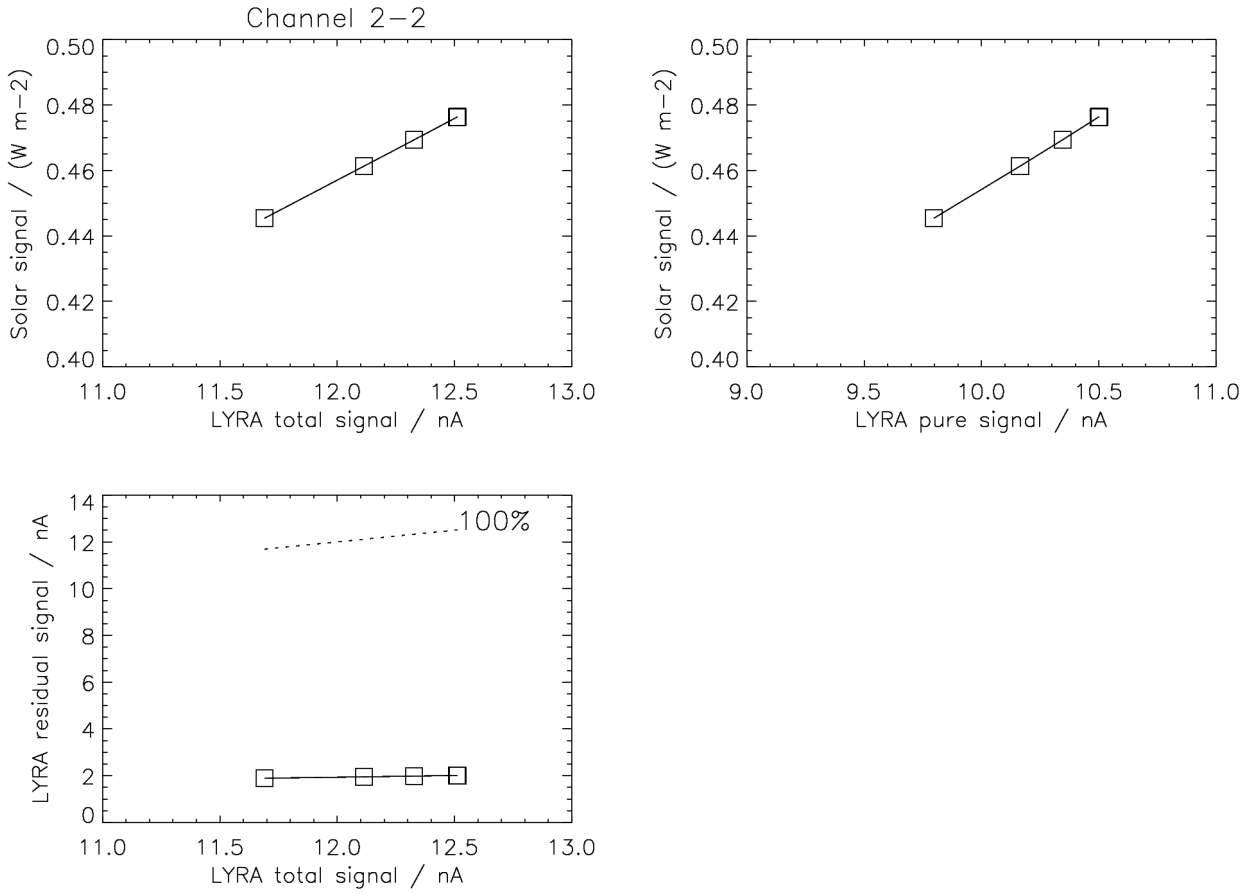

Figure 2-2a. Simulated relations between input and output for LYRA channel 2-2.

Remarks: The behavior of samples pre1, fla1, pre2, fla2 is approx. identical, thus there are only four significantly different data points. Please note the consequence for channel 2-1: While there is a different total and pure (Lyman-alpha) signal response for the last four samples, i.e. pre1,fla1 vs. pre2,fla2, the residual signal is approx. identical, because it is dominated by longer wavelengths - like the channel 2-2 signal shown here.

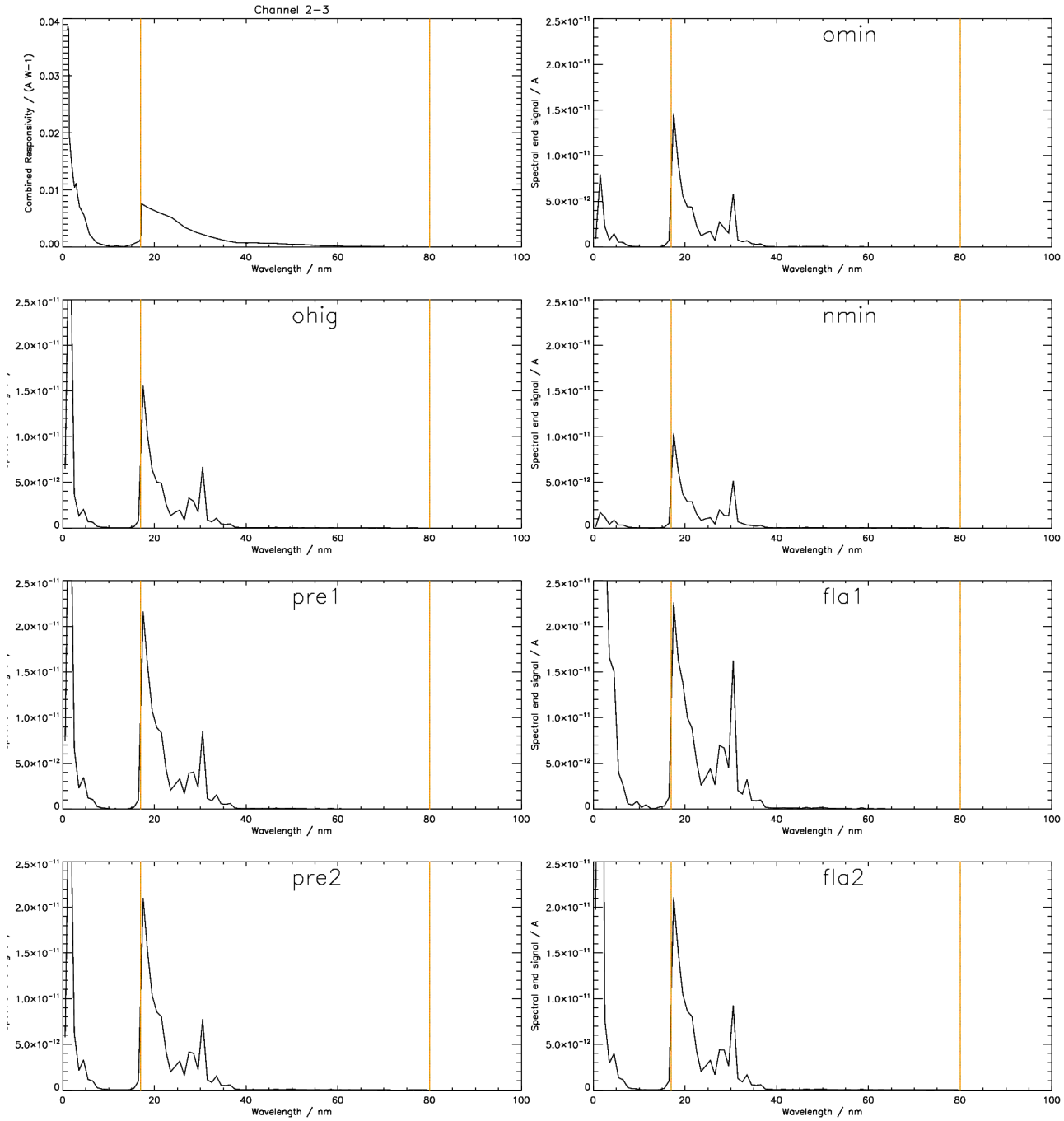

Figure 2-3. Measured responsivity and simulated output for LYRA channel 2-3
Aluminium + MSM15 (17-80 nm)

sample	total	pure	residual	solar
omin	0.0769017 nA	0.0614796 nA (79.9%)	0.0154221 nA	0.00225541 Wm-2
ohig	0.124030 nA	0.0696541 nA (56.2%)	0.0543756 nA	0.00263286 Wm-2
nmin	0.0493309 nA	0.0436954 nA (88.6%)	0.0056355 nA	0.00171904 Wm-2
pre1	0.172380 nA	0.104411 nA (60.6%)	0.0679689 nA	0.00376518 Wm-2
fla1	1.74479 nA	0.136178 nA (7.8%)	1.60861 nA	0.00570166 Wm-2
pre2	0.161834 nA	0.100741 nA (62.2%)	0.0610935 nA	0.00362499 Wm-2
fla2	0.249393 nA	0.104520 nA (41.9%)	0.144872 nA	0.00394254 Wm-2

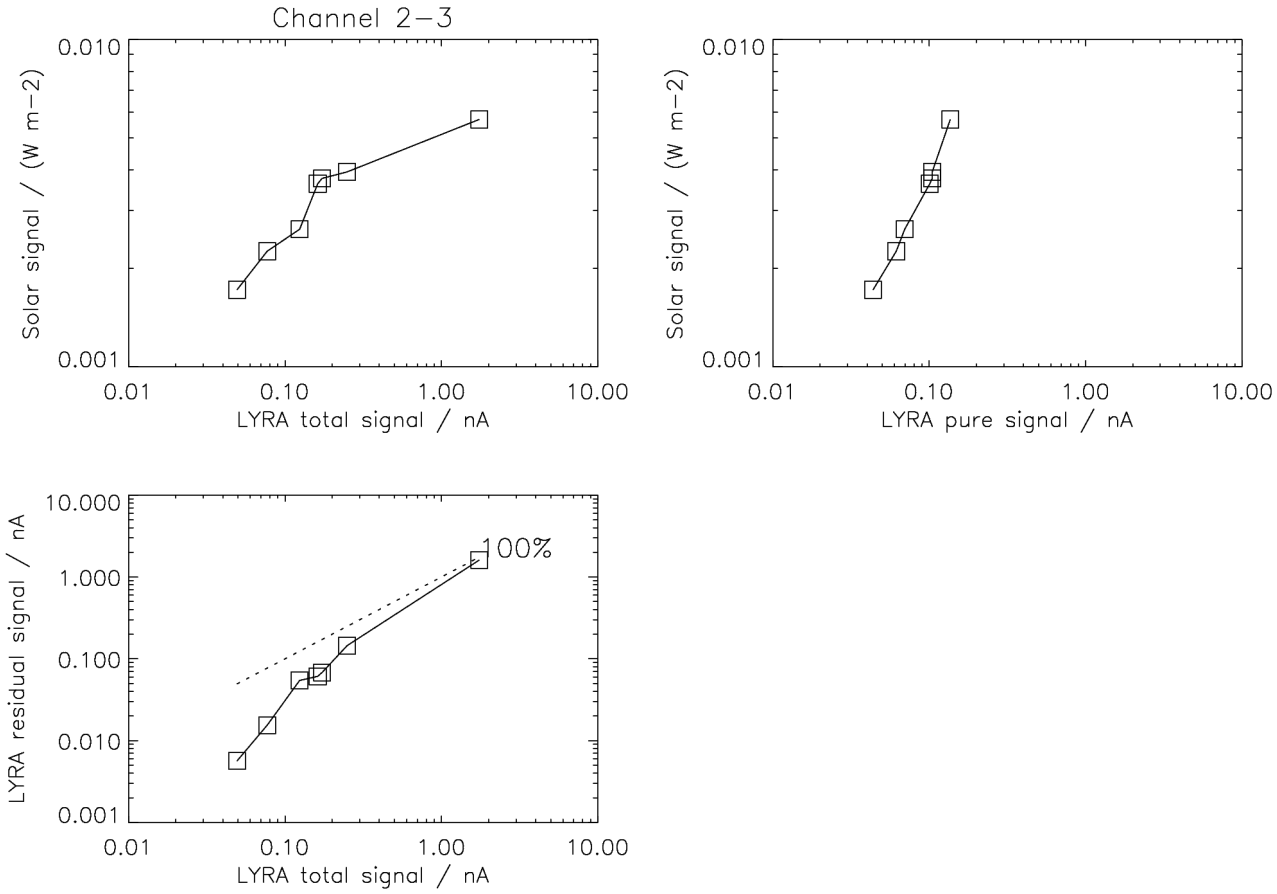

Figure 2-3a. Simulated relations between input and output for LYRA channel 2-3.

Remarks: The functional relation between the solar signal and the LYRA total signal is still not quite straightforward (but much less irregular than before the "new-spectra" update, compare upper left image before and after). The reason for nonlinearity is a contamination due to the influence of the interval below ~10 nm, which is not part of the 17-80 nm nominal interval of the Al channels. - Although the channel interval nominally reaches up to 80 nm, effectively it appears to end at 35 nm (see Figure 2-3). - For the small subset of flare events, the uncalibrated data of this channel (i.e. before subtraction of the substantial short-wavelength contamination) will probably not be very meaningful.

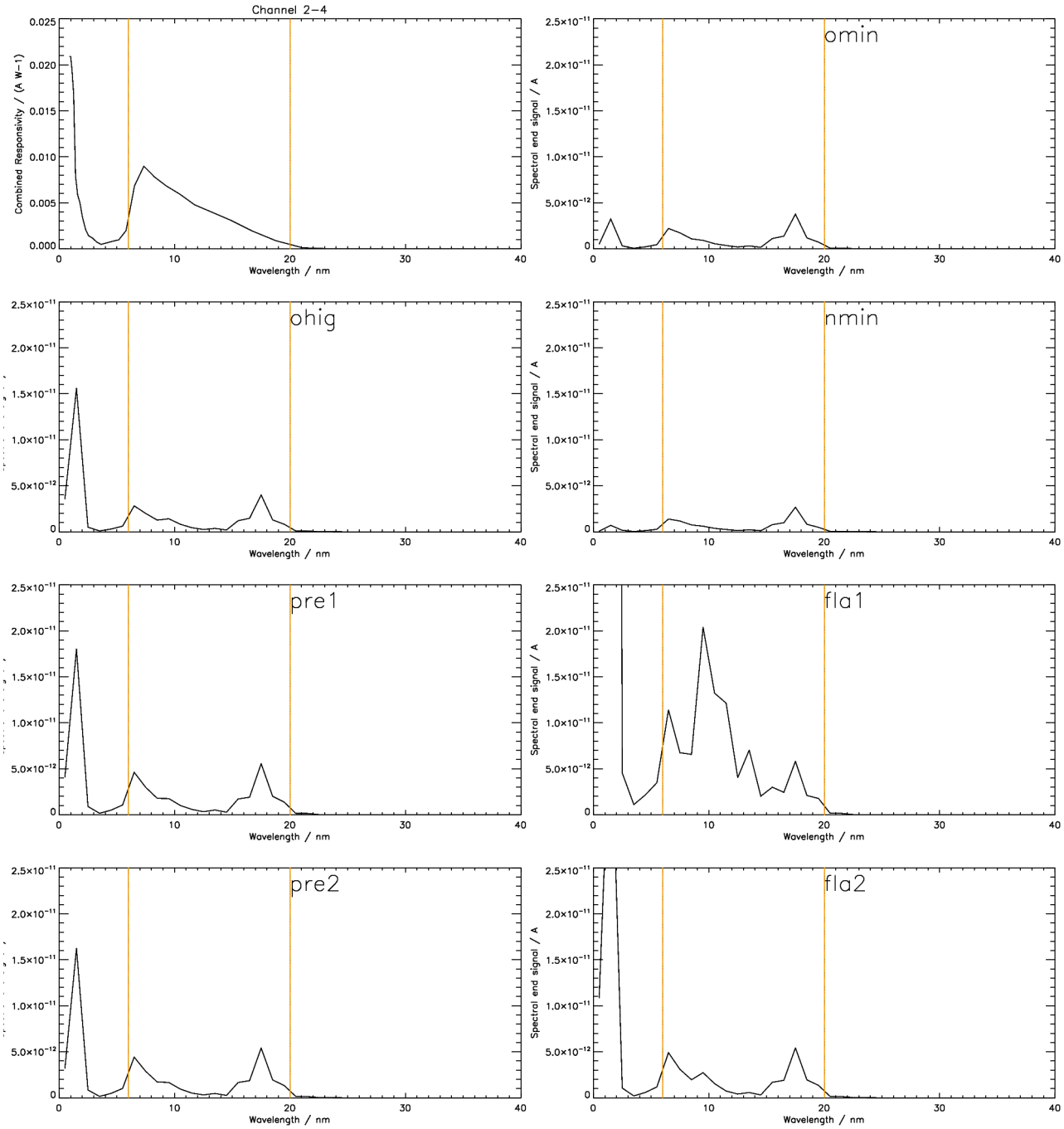

Figure 2-4. Measured responsivity and simulated output for LYRA channel 2-4
Zr(150nm) + MSM19 (6-20 nm)

sample	total	pure	residual	solar
omin	0.0207628 nA	0.0155704 nA (75.0%)	0.00519240 nA	0.00088964 Wm-2
ohig	0.0393822 nA	0.0182603 nA (46.4%)	0.0211220 nA	0.00099602 Wm-2
nmin	0.0123416 nA	0.0106228 nA (86.1%)	0.00171875 nA	0.00061296 Wm-2
pre1	0.0516737 nA	0.0263599 nA (51.0%)	0.0253138 nA	0.00146242 Wm-2
fla1	0.786811 nA	0.0986240 nA (12.5%)	0.688187 nA	0.00340528 Wm-2
pre2	0.0477878 nA	0.0253012 nA (52.9%)	0.0224866 nA	0.00141076 Wm-2
fla2	0.0861456 nA	0.0284688 nA (33.0%)	0.0576768 nA	0.00148986 Wm-2

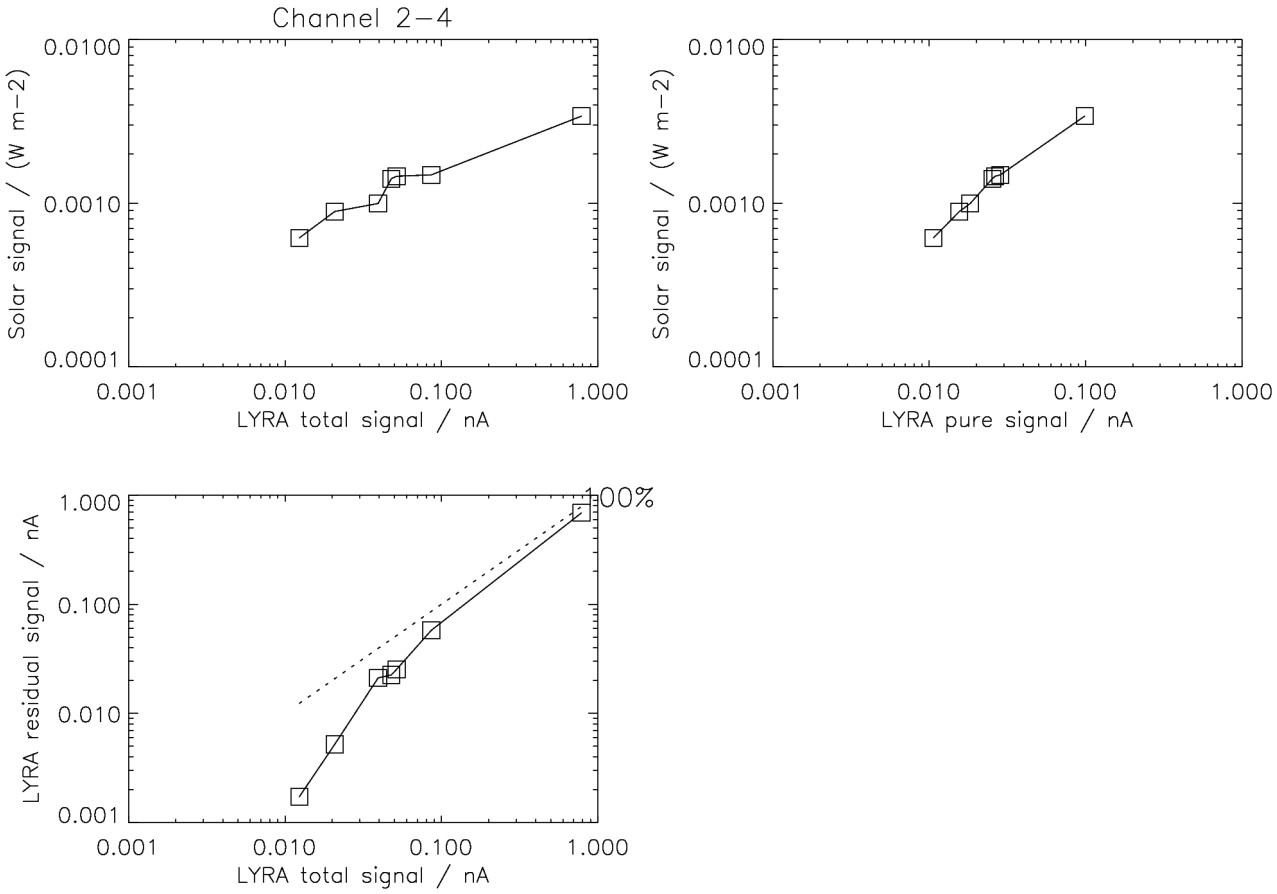

Figure 2-4a. Simulated relations between input and output for LYRA channel 2-4.

Remarks: After redefining the nominal interval of the Zr channel, the functional relation between the solar signal and the LYRA total signal is not straightforward any more, but rather resembles the Al channel. The reason for nonlinearity is a contamination due to the influence of the interval below ~3 nm, which is not part of the new 6-20 nm nominal interval of the Zr channels. - For the small subset of flare events, the uncalibrated data of this channel (i.e. before subtraction of the substantial short-wavelength contamination) will probably not be very meaningful.

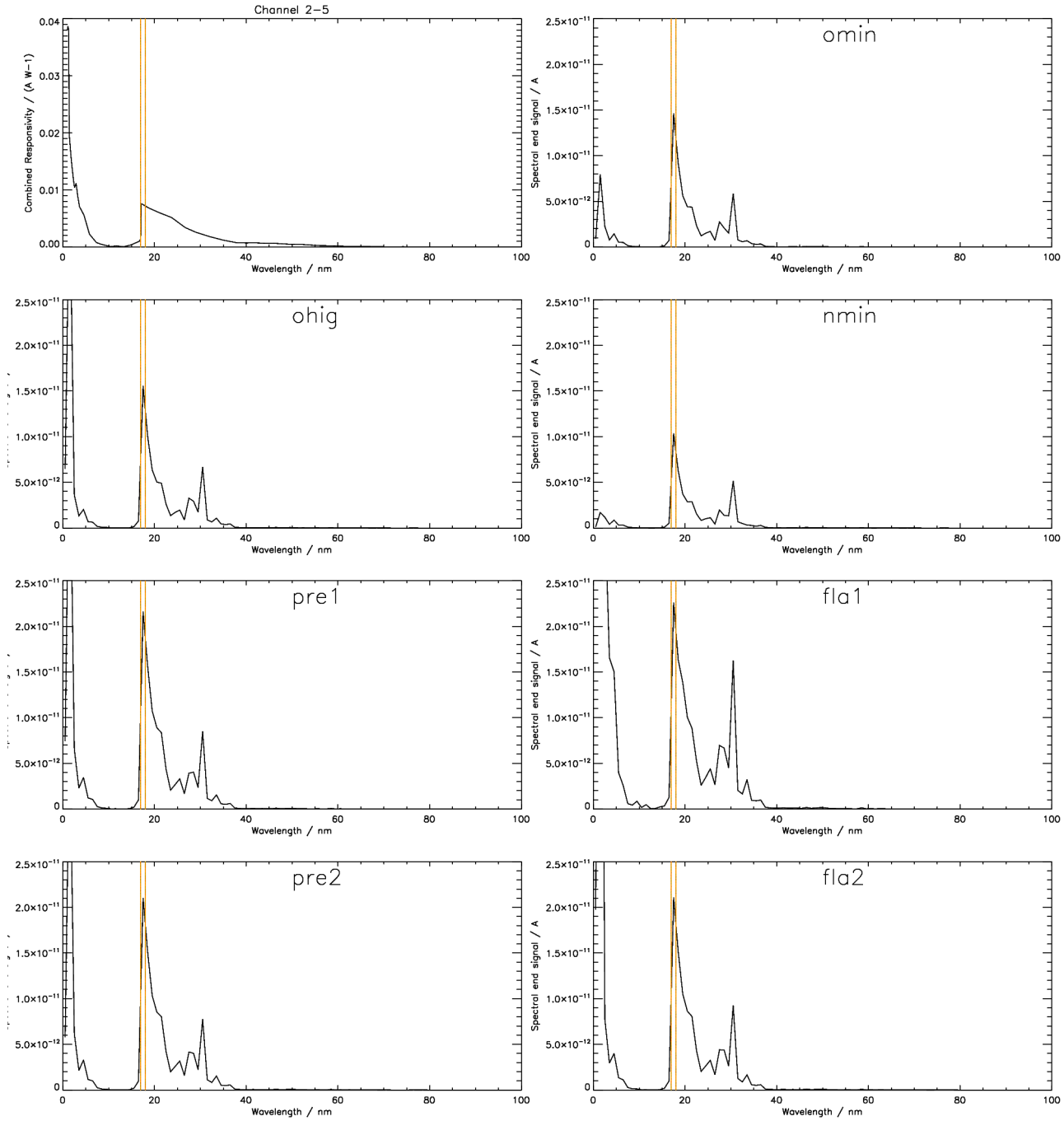

Figure 2-5. Measured responsivity and simulated output for the *virtual* LYRA channel 2-5 Aluminium + MSM15 *(17-18 nm, for cross-calibration with SWAP)*

sample	total	pure	residual	solar
omin	0.0769017 nA	0.0146279 nA (19.0%)	0.0622737 nA	0.000274049 Wm-2
ohig	0.124030 nA	0.0155522 nA (12.5%)	0.108478 nA	0.000291364 Wm-2
nmin	0.0493309 nA	0.0103526 nA (21.0%)	0.0389783 nA	0.000193953 Wm-2
pre1	0.172380 nA	0.0215976 nA (12.5%)	0.150782 nA	0.000404624 Wm-2
fla1	1.74479 nA	0.0226003 nA (1.3%)	1.72219 nA	0.000423409 Wm-2
pre2	0.161834 nA	0.0210362 nA (13.0%)	0.140798 nA	0.000394106 Wm-2
fla2	0.249393 nA	0.0210843 nA (8.5%)	0.228308 nA	0.000395006 Wm-2

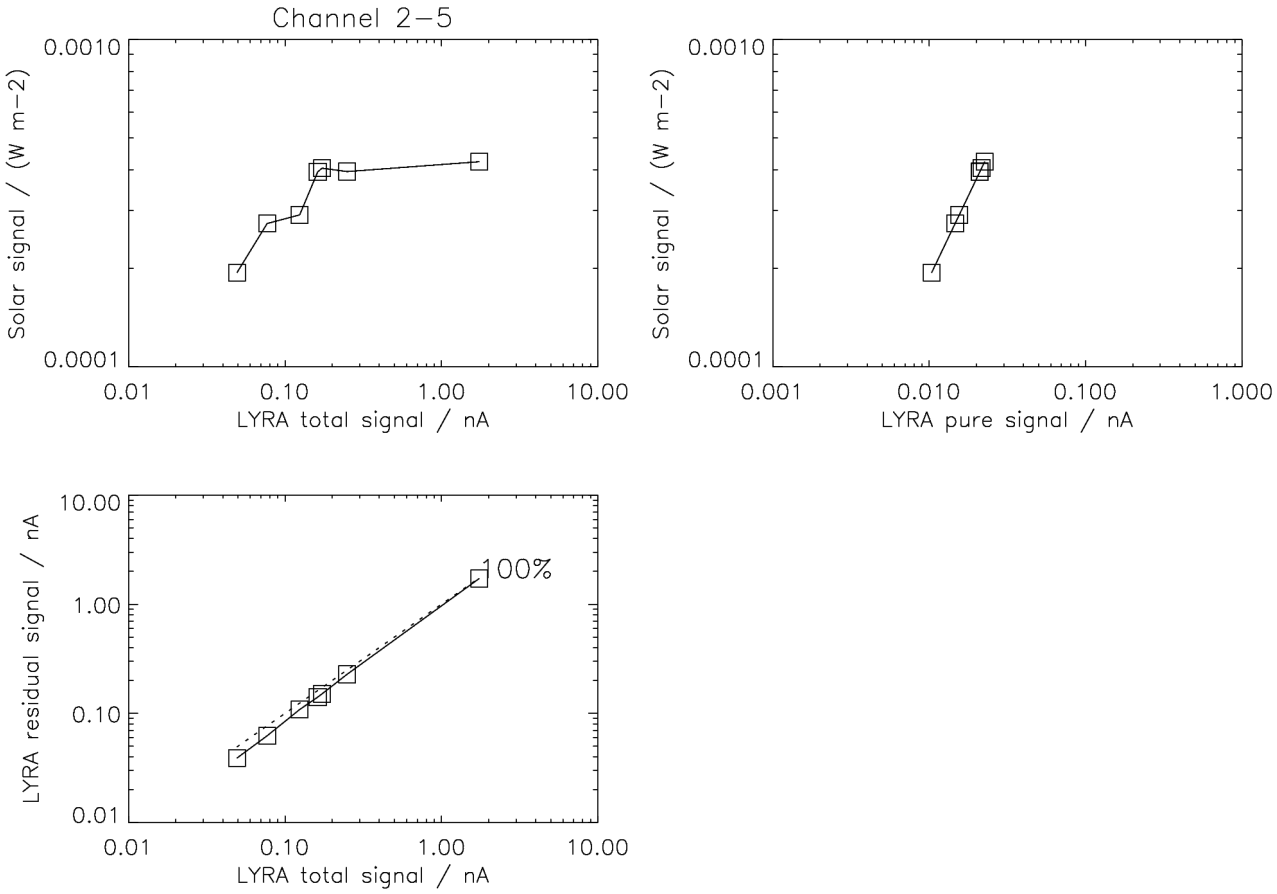

Figure 2-5a. Simulated relations between input and output for *virtual* LYRA channel 2-5.

Remarks: The functional relation between the (SWAP) solar signal and the LYRA total signal is not straightforward. One reason for nonlinearity is a contamination due to the influence of the interval below ~10 nm. It appears that a flare will hardly influence the solar irradiance as measured by SWAP.

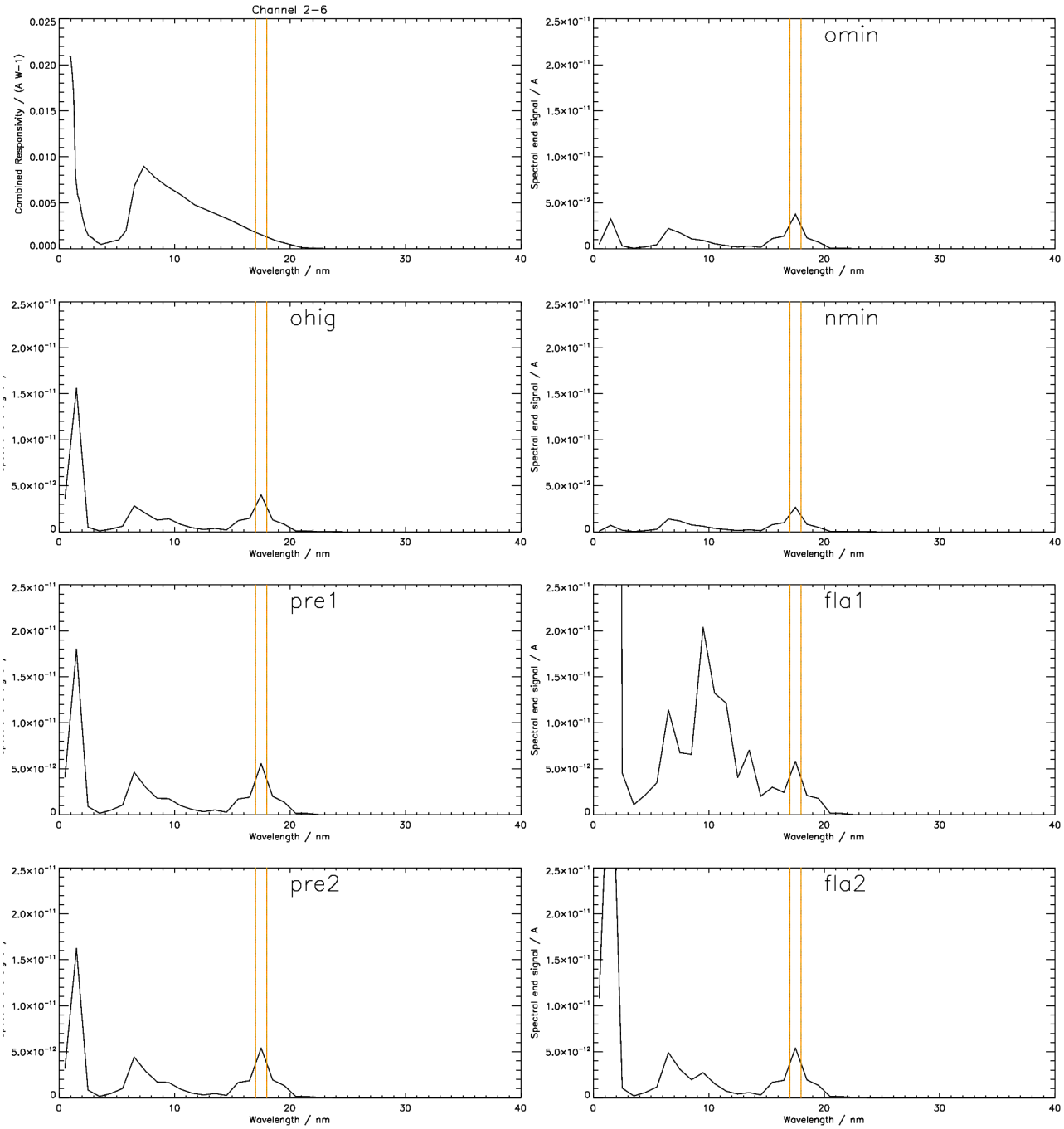

Figure 2-6. Measured responsivity and simulated output for the *virtual* LYRA channel 2-6 Zr(150nm) + MSM19 *(17-18 nm, for cross-calibration with SWAP)*

sample	total	pure	residual	solar
omin	0.0207628 nA	0.0037614 nA (18.1%)	0.0170014 nA	0.000274049 Wm-2
ohig	0.0393822 nA	0.0039991 nA (10.2%)	0.0353832 nA	0.000291364 Wm-2
nmin	0.0123416 nA	0.0026621 nA (21.6%)	0.00967947 nA	0.000193953 Wm-2
pre1	0.0516737 nA	0.0055536 nA (10.7%)	0.0461201 nA	0.000404624 Wm-2
fla1	0.786811 nA	0.0058115 nA (0.7%)	0.781000 nA	0.000423409 Wm-2
pre2	0.0477878 nA	0.0054093 nA (11.3%)	0.0423785 nA	0.000394106 Wm-2
fla2	0.0861456 nA	0.0054216 nA (6.3%)	0.0807240 nA	0.000395006 Wm-2

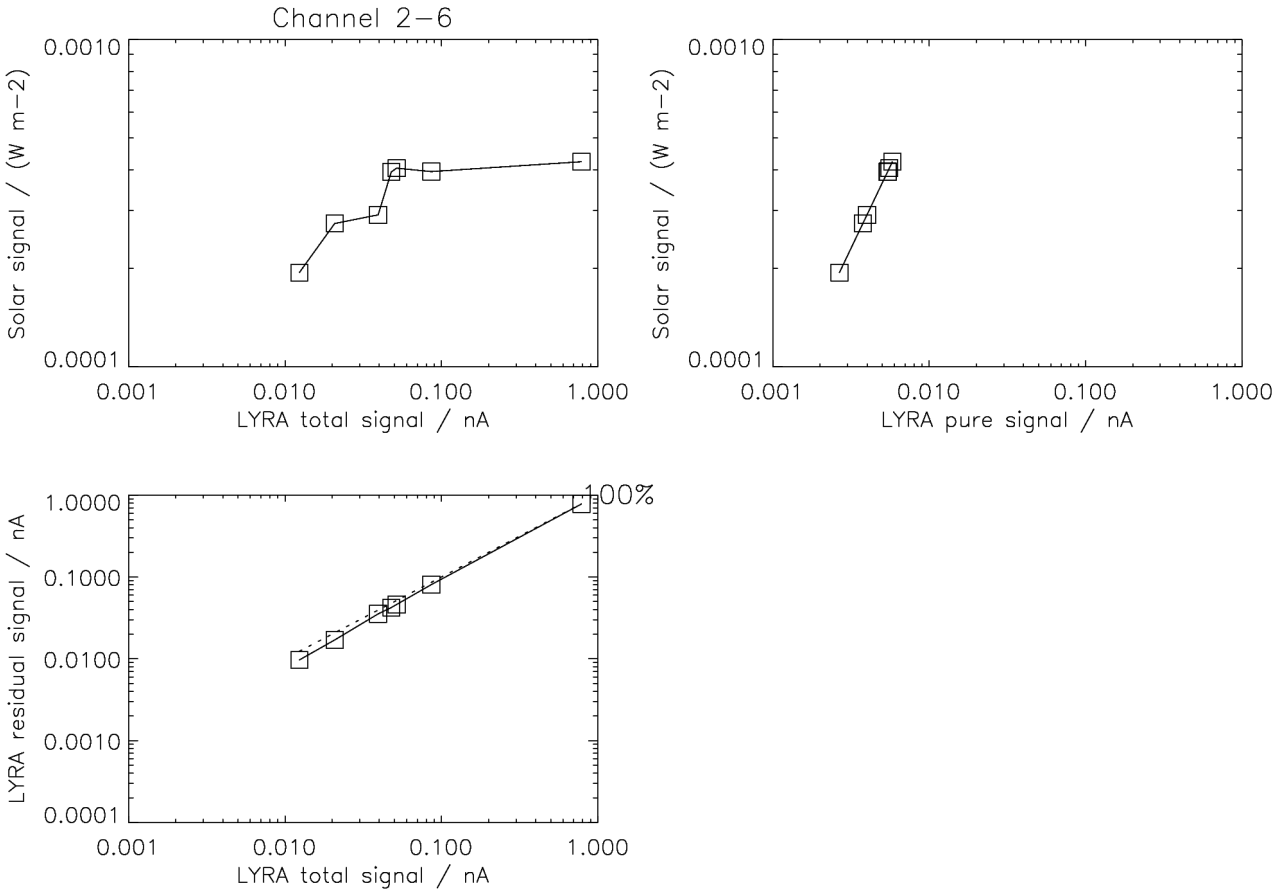

Figure 2-6a. Simulated relations between input and output for *virtual* LYRA channel 2-6.

Remarks: The functional relation between the (SWAP) solar signal and the LYRA total signal is not straightforward. One reason for nonlinearity is a contamination due to the influence of the interval below ~3 nm. It appears that a flare will hardly influence the solar irradiance as measured by SWAP.

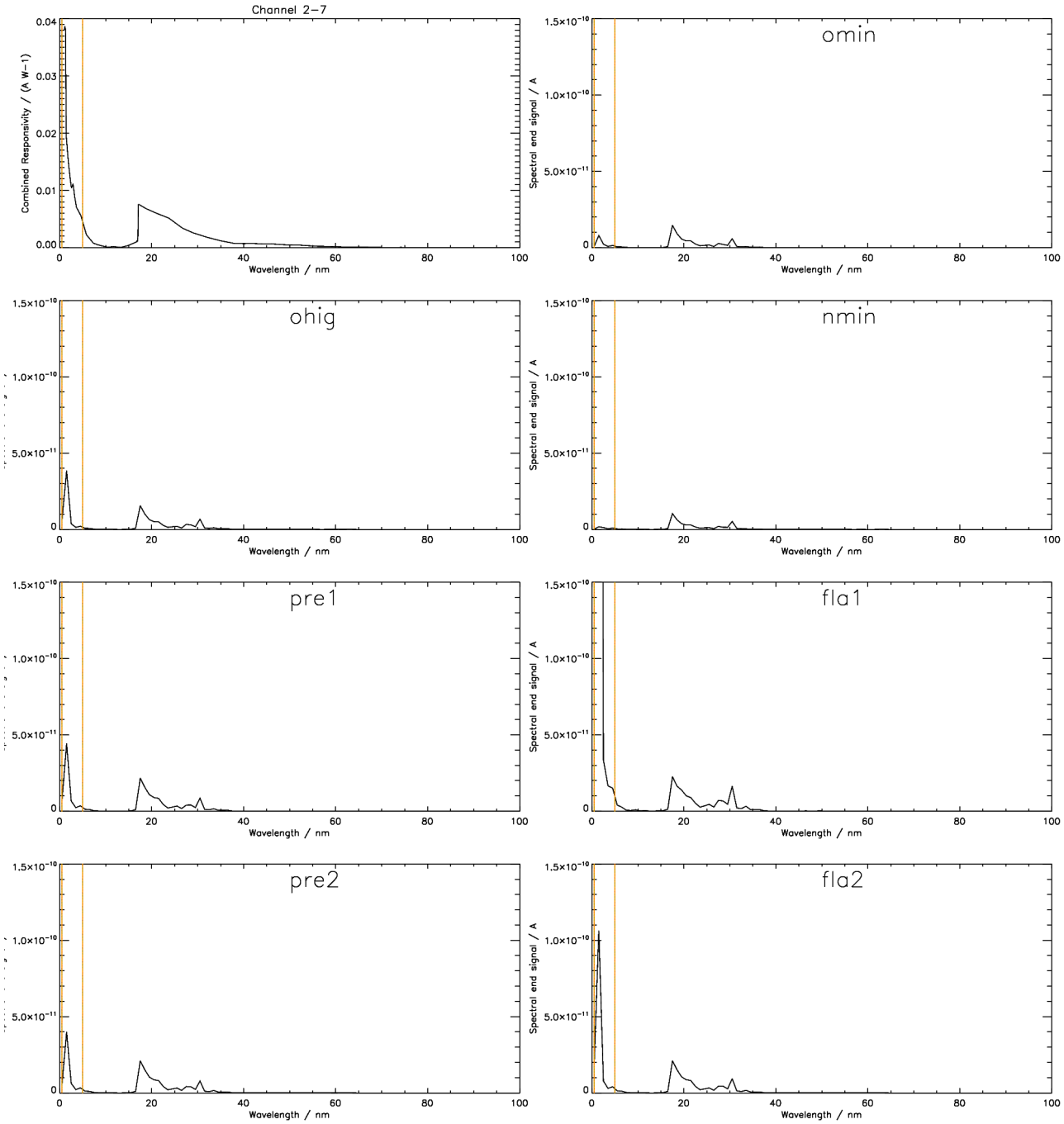

Figure 2-7. Measured responsivity and simulated output for the *virtual* LYRA channel 2-7
Aluminium + MSM15 *(< 5 nm, for cross-calibration with TIMED/SEE, or additional product?)*

sample	total	pure	residual	solar
omin	0.0769017 nA	0.0132928 nA (17.3%)	0.0636089 nA	0.000143220 Wm-2
ohig	0.124030 nA	0.0518015 nA (41.8%)	0.0722282 nA	0.000430065 Wm-2
nmin	0.0493309 nA	0.0042293 nA (8.6%)	0.0451016 nA	0.0000581368 Wm-2
pre1	0.172380 nA	0.0640376 nA (37.1%)	0.108342 nA	0.000572517 Wm-2
fla1	1.74479 nA	1.59772 nA (91.6%)	0.147069 nA	0.0109987 Wm-2
pre2	0.161834 nA	0.0573168 nA (35.4%)	0.104518 nA	0.000521914 Wm-2
fla2	0.249393 nA	0.140677 nA (56.4%)	0.108716 nA	0.00111161 Wm-2

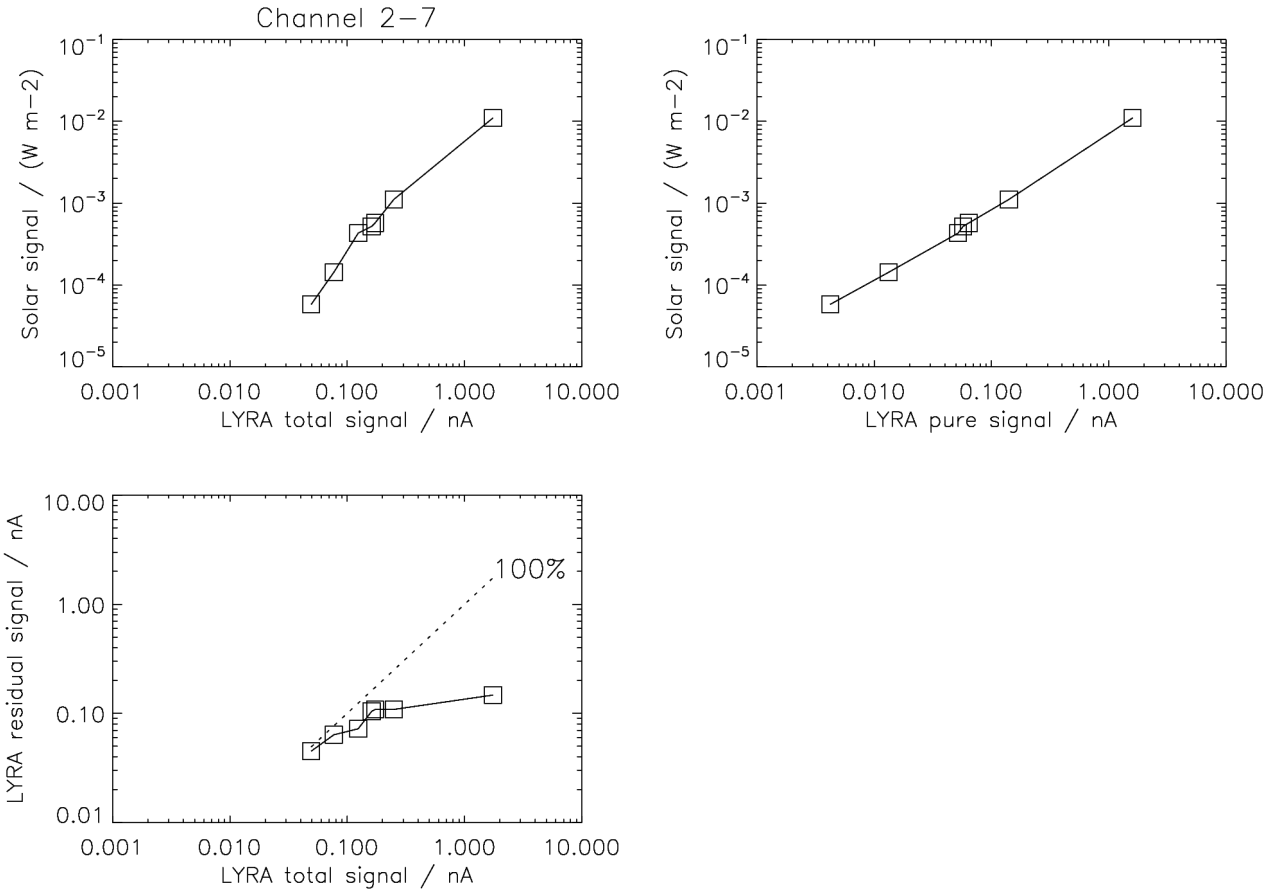

Figure 2-7a. Simulated relations between input and output for *virtual* LYRA channel 2-7.

Remarks: The functional relation between the (< 5 nm, SXR) solar signal and the LYRA total signal is not straightforward, because (a) the channel's responsivity is higher for short wavelengths, and (b) the EUV signal dominates in non-flare situations.

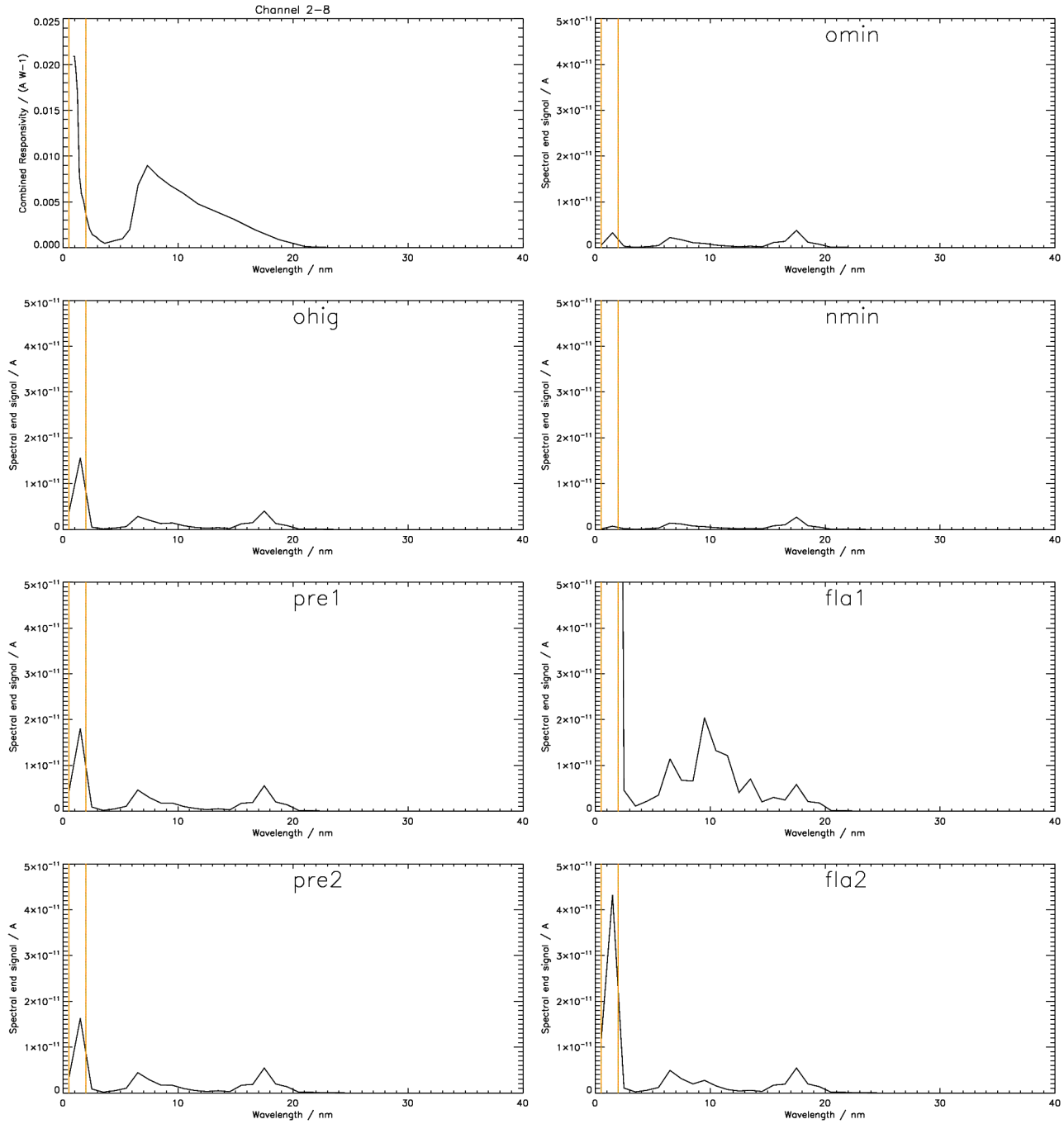

Figure 2-8. Measured responsivity and simulated output for the *virtual* LYRA channel 2-8
Zr(150nm) + MSM19 *(< 2 nm, for cross-calibration with TIMED/SEE, or additional product?)*

sample	total	pure	residual	solar
omin	0.0207628 nA	0.0037333 nA (18.0%)	0.0170296 nA	0.0000611985 Wm-2
ohig	0.0393822 nA	0.0191679 nA (48.7%)	0.0202144 nA	0.000303303 Wm-2
nmin	0.0123416 nA	0.0007554 nA (6.1%)	0.0115862 nA	0.0000127735 Wm-2
pre1	0.0516737 nA	0.0221017 nA (42.8%)	0.0295720 nA	0.000350038 Wm-2
fla1	0.786811 nA	0.676271 nA (86.0%)	0.110540 nA	0.00983327 Wm-2
pre2	0.0477878 nA	0.0194258 nA (40.7%)	0.0283620 nA	0.000312139 Wm-2
fla2	0.0861456 nA	0.0540825 nA (62.8%)	0.0320631 nA	0.000846606 Wm-2

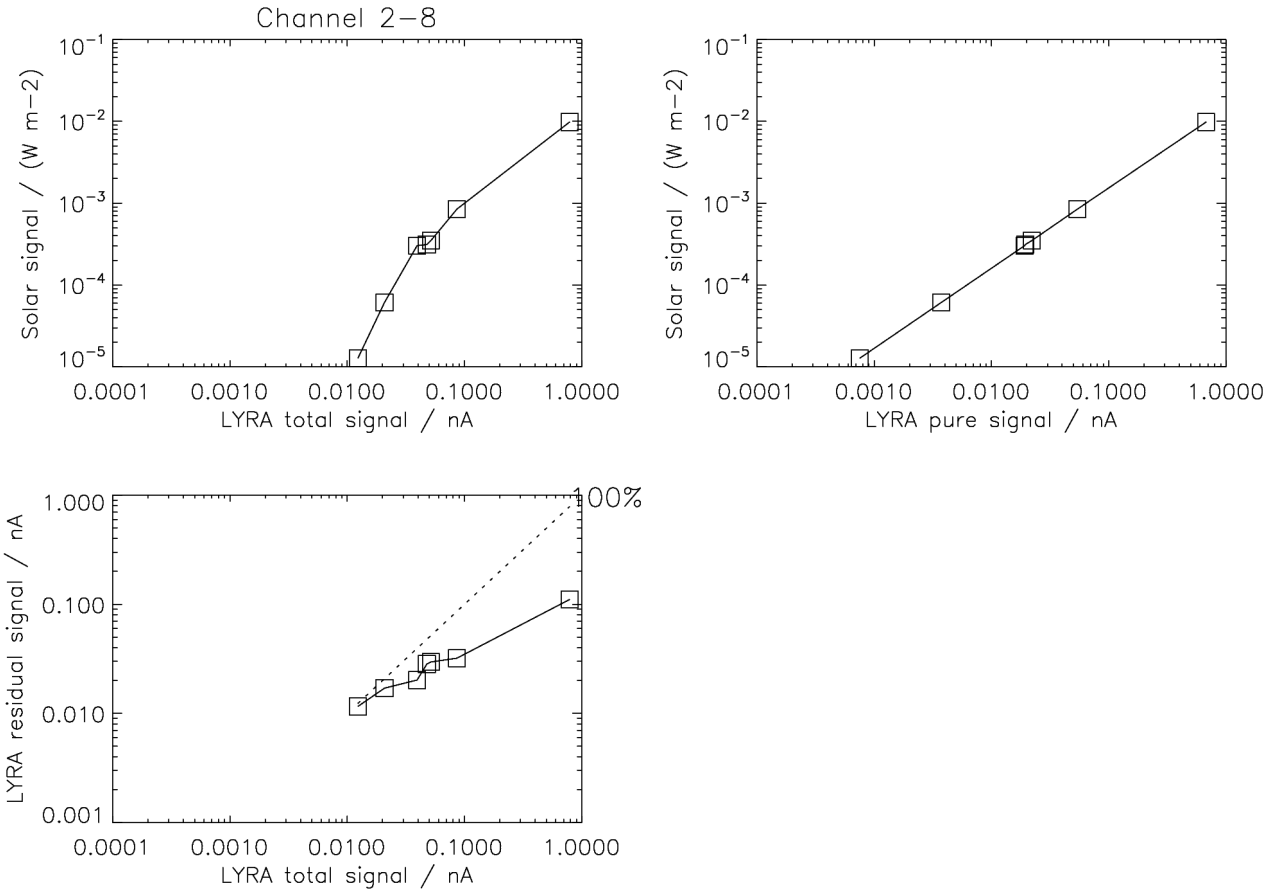

Figure 2-8a. Simulated relations between input and output for *virtual* LYRA channel 2-8.

Remarks: The functional relation between the (< 2 nm, SXR) solar signal and the LYRA total signal is not straightforward, because (a) the channel's responsivity is higher for short wavelengths, and (b) the EUV signal dominates in non-flare situations.

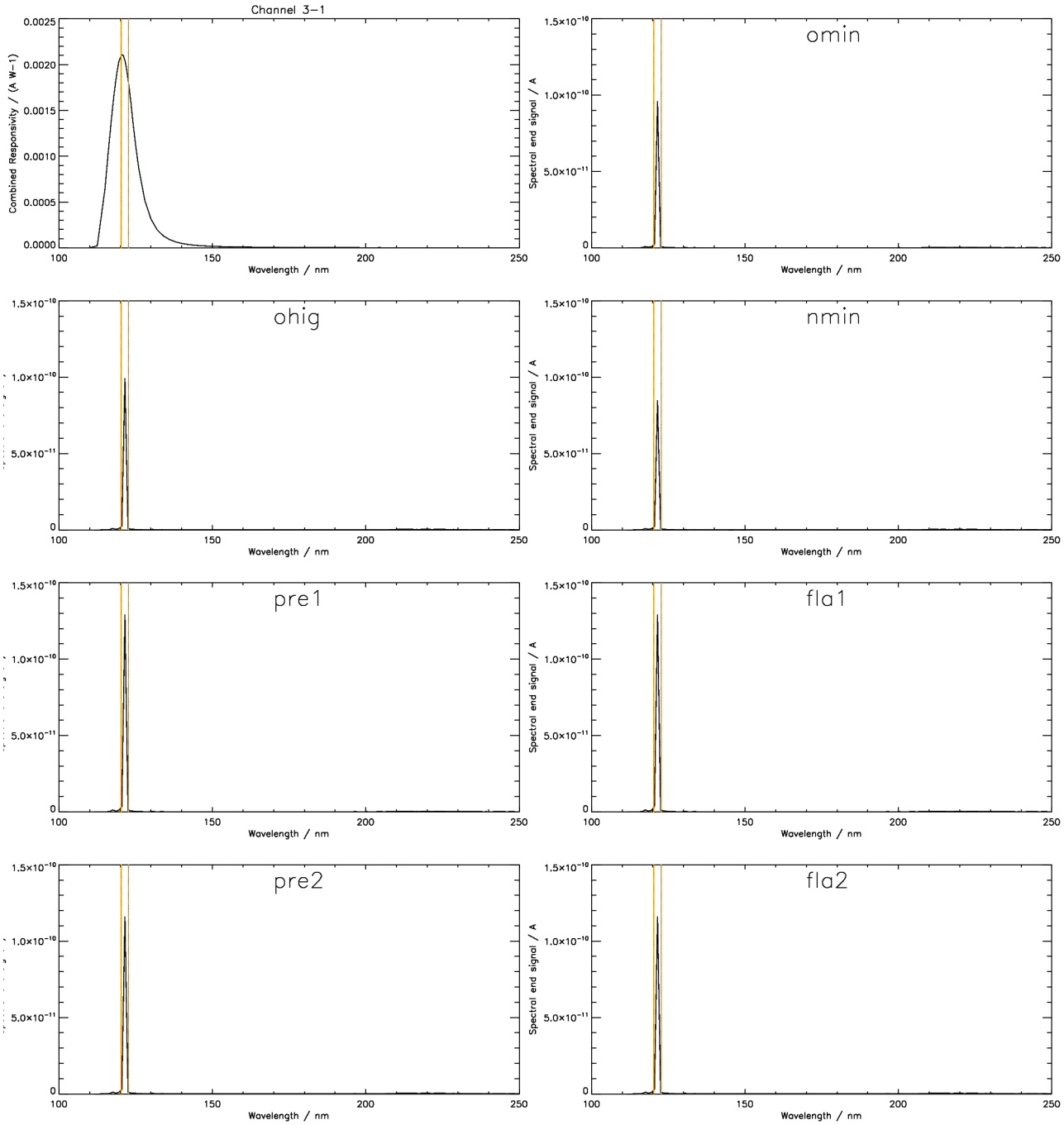

Figure 3-1. Measured responsivity and simulated output for LYRA channel 3-1
Ly N+XN + AXUV20A (121.5 +/- nm)

sample	total	pure	residual	solar
omin	0.281382 nA	0.0990736 nA (35.2%)	0.182308 nA	0.00690130 Wm-2
ohig	0.284792 nA	0.102585 nA (36.0%)	0.182208 nA	0.00714568 Wm-2
nmin	0.269455 nA	0.0876394 nA (32.5%)	0.181816 nA	0.00610500 Wm-2
pre1	0.317185 nA	0.133704 nA (42.2%)	0.183481 nA	0.00931232 Wm-2
fla1	0.317211 nA	0.133704 nA (42.1%)	0.183507 nA	0.00931232 Wm-2
pre2	0.303240 nA	0.120042 nA (39.6%)	0.183198 nA	0.00836111 Wm-2
fla2	0.303248 nA	0.120042 nA (39.6%)	0.183206 nA	0.00836111 Wm-2

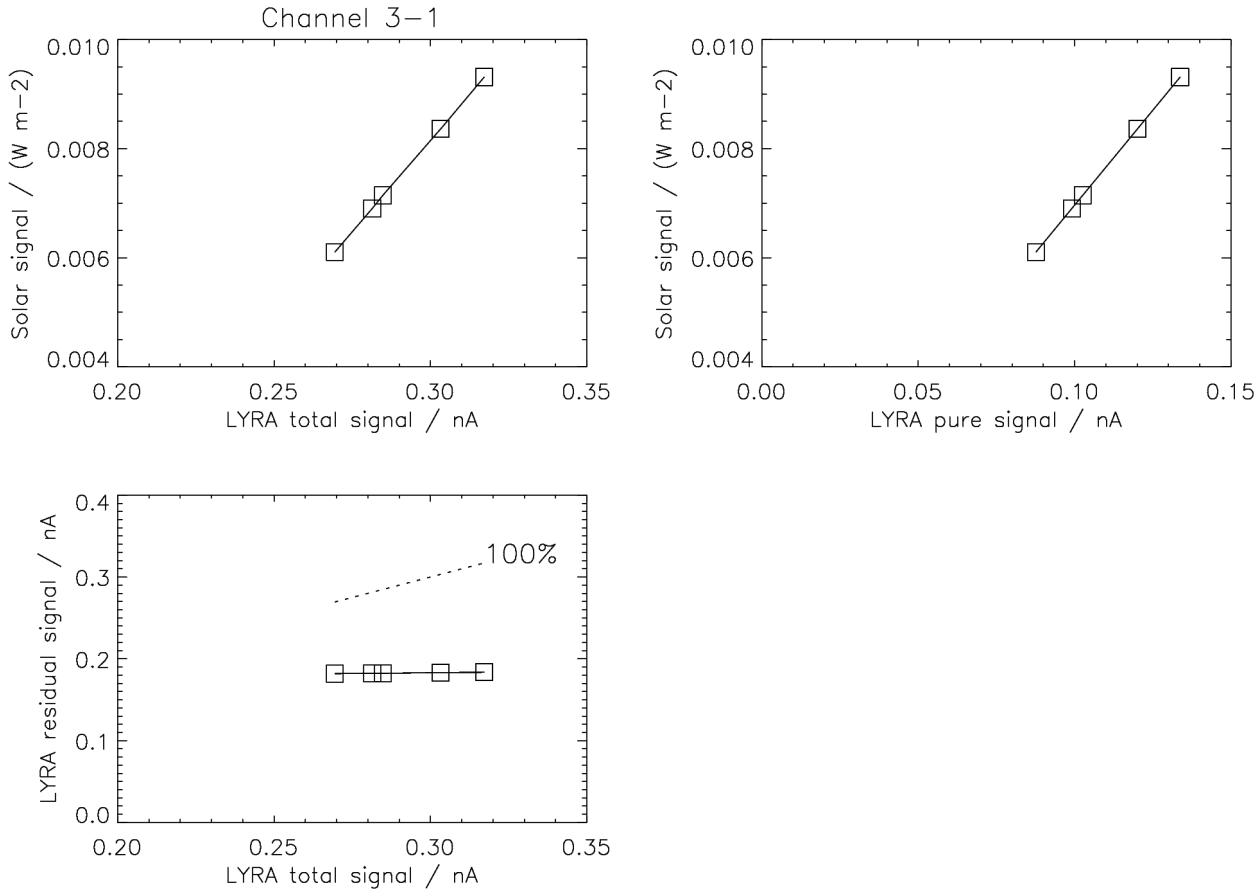

Figure 3-1a. Simulated relations between input and output for LYRA channel 3-1.

Remarks: Defining 2.5 nm around 121.5 nm as nominal interval leads to just three SORCE data points (120.5, 121.5, and 122.5 nm), of which only 121.5 nm is significant. This means that the simulation is essentially based on one value; a small variation of the nominal interval would not lead to different simulation results. - The functional relation between the solar signal and the LYRA total signal is almost linear (see upper left image). The residual signal must be a contamination due to the influence of the visual and infrared. Other than in channel 1-1 and 1-2, there is no contamination between 200-230 nm, thus the residual signal can be assumed to be almost constant.

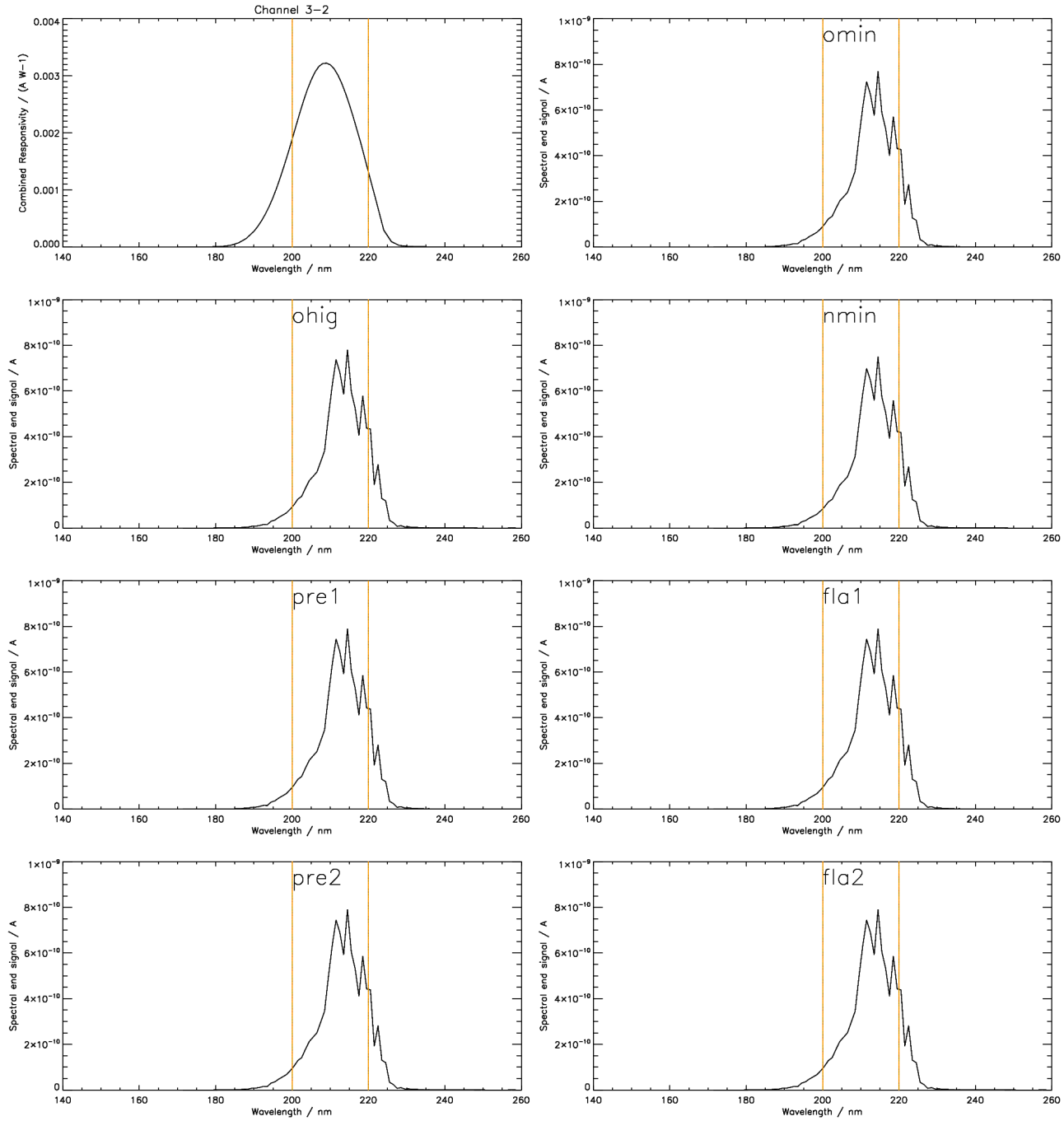

Figure 3-2. Measured responsivity and simulated output for LYRA channel 3-2
Herzberg + PIN12 (200-220 nm)

sample	total	pure	residual	solar
omin	9.73290 nA	8.13731 nA (83.6%)	1.59559 nA	0.461334 Wm-2
ohig	9.90543 nA	8.28307 nA (83.6%)	1.62236 nA	0.469345 Wm-2
nmin	9.38879 nA	7.84033 nA (83.5%)	1.54846 nA	0.445404 Wm-2
pre1	10.0549 nA	8.40909 nA (83.6%)	1.64580 nA	0.476369 Wm-2
fla1	10.0549 nA	8.40909 nA (83.6%)	1.64580 nA	0.476369 Wm-2
pre2	10.0529 nA	8.40616 nA (83.6%)	1.64677 nA	0.476294 Wm-2
fla2	10.0529 nA	8.40616 nA (83.6%)	1.64677 nA	0.476294 Wm-2

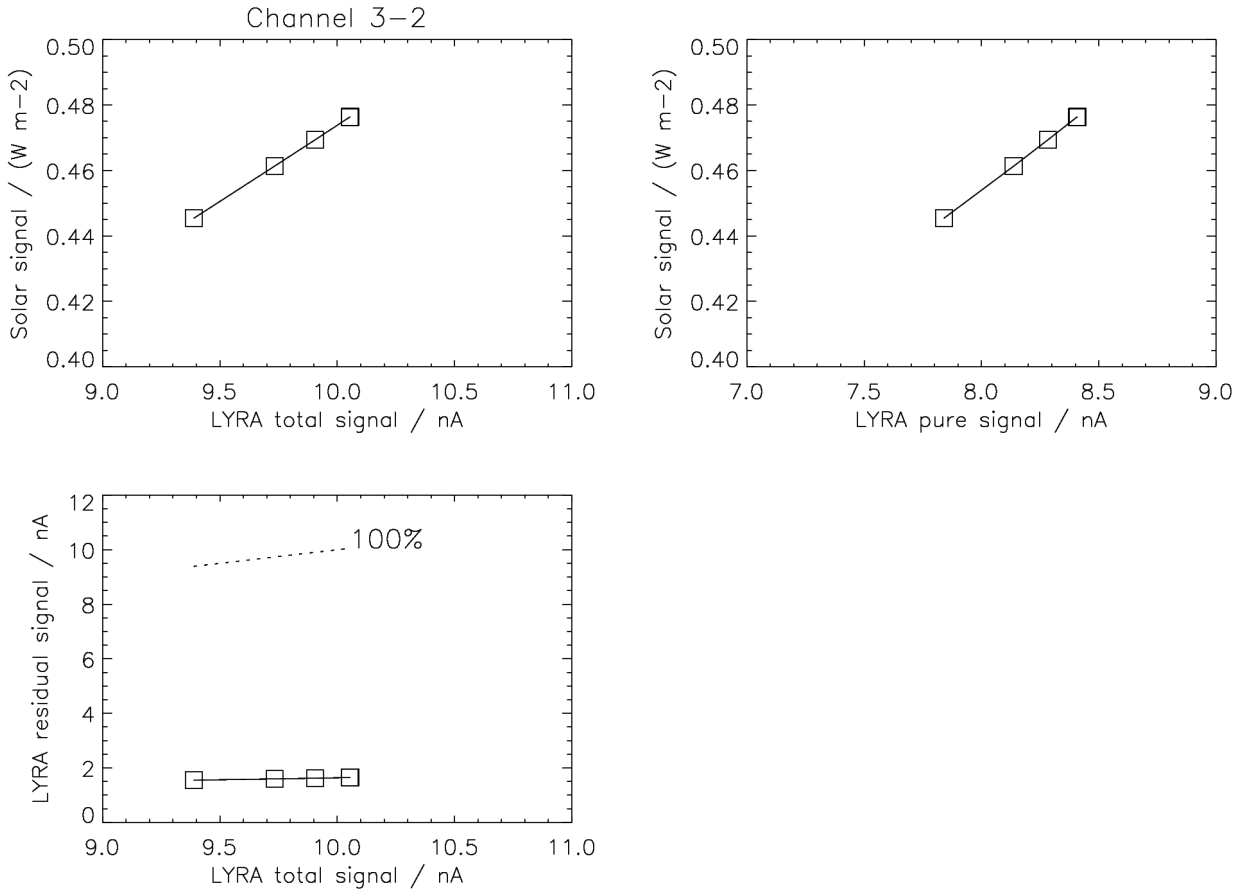

Figure 3-2a. Simulated relations between input and output for LYRA channel 3-2.

The behavior of samples pre1, fla1, pre2, fla2 is approx. identical, thus there are only four significantly different data points. Please note the consequence for channel 3-1: While there is a different total and pure (Lyman-alpha) signal response for the last four samples, i.e. pre1,fla1 vs. pre2,fla2, the residual signal is approx. identical, because it is dominated by longer wavelengths - like the channel 3-2 signal. (This argument is weaker here than for channels 1-1 and 2-1, though, since in 3-1 the residual is approx. the same in *all* cases; see above.)

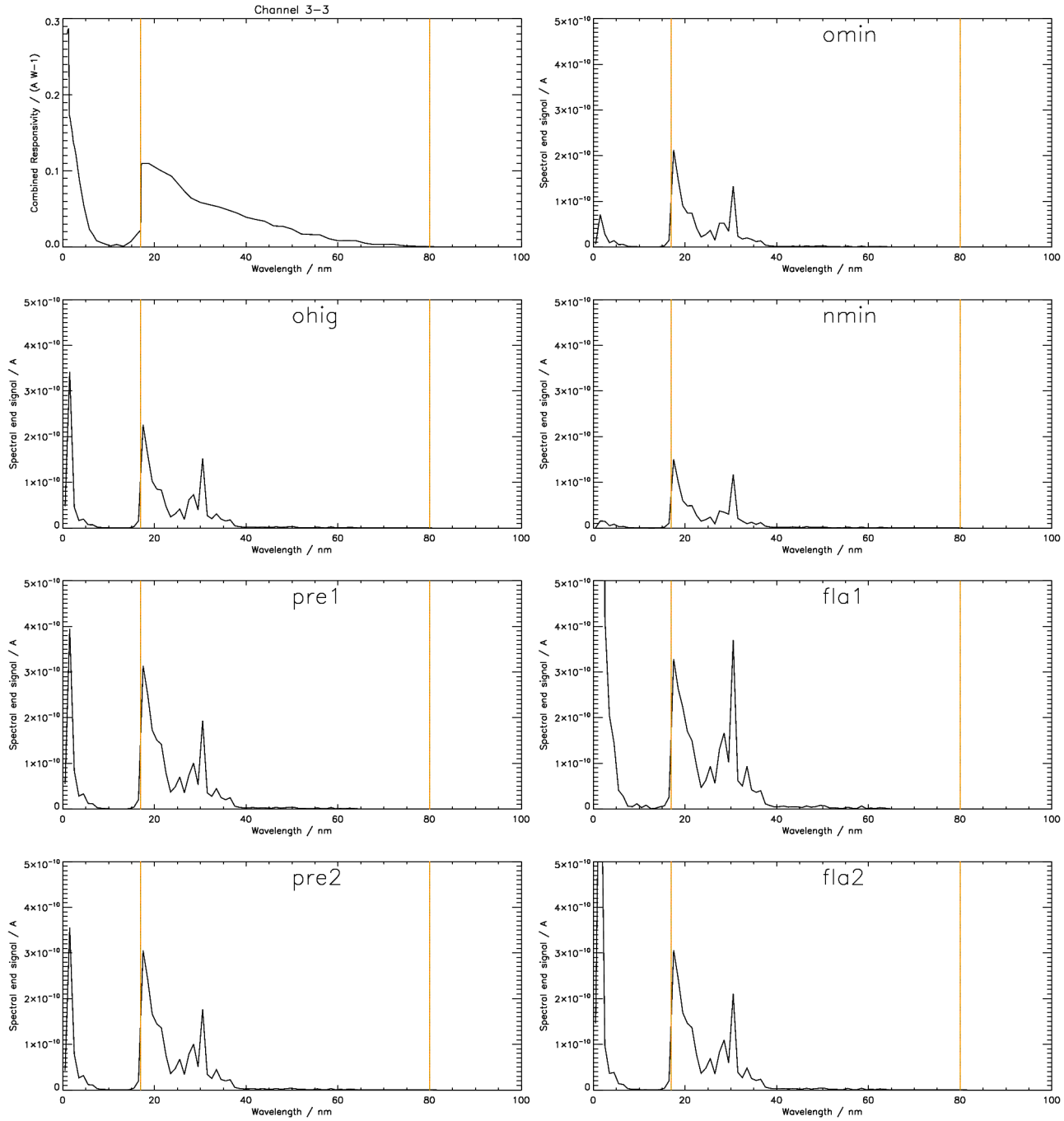

Figure 3-3. Measured responsivity and simulated output for LYRA channel 3-3.
Aluminium + AXUV20B (17-80 nm)

sample	total	pure	residual	solar
omin	1.32016 nA	1.15029 nA (87.1%)	0.169869 nA	0.00225541 Wm-2
ohig	1.83762 nA	1.32039 nA (71.9%)	0.517229 nA	0.00263286 Wm-2
nmin	0.906568 nA	0.832055 nA (91.8%)	0.0745133 nA	0.00171904 Wm-2
pre1	2.61304 nA	1.95557 nA (74.8%)	0.657466 nA	0.00376518 Wm-2
fla1	16.7010 nA	2.69202 nA (16.1%)	14.0090 nA	0.00570166 Wm-2
pre2	2.47889 nA	1.88284 nA (76.0%)	0.596046 nA	0.00362499 Wm-2
fla2	3.30640 nA	1.97520 nA (59.7%)	1.33120 nA	0.00394254 Wm-2

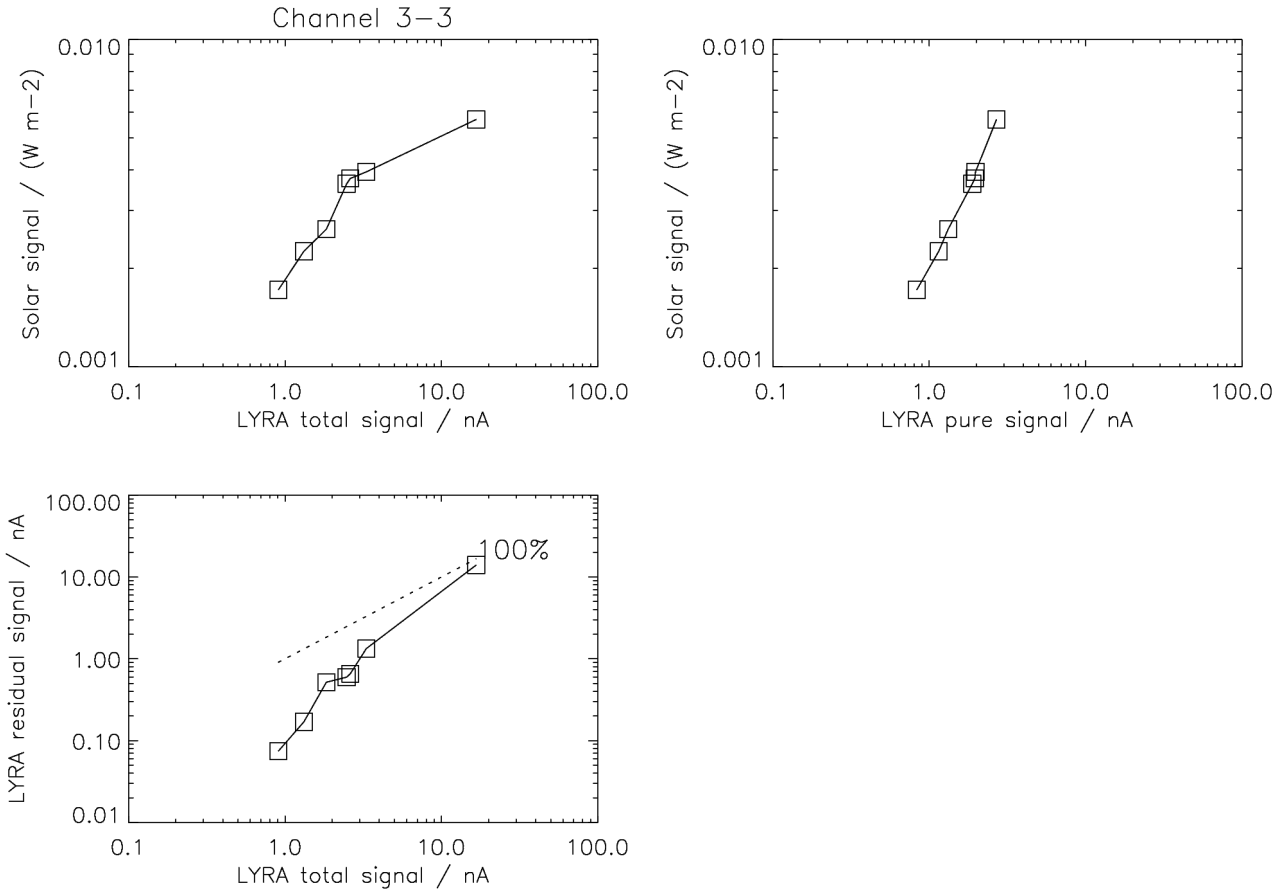

Figure 3-3a. Simulated relations between input and output for LYRA channel 3-3.

Remarks: The functional relation between the solar signal and the LYRA total signal is still not quite straightforward (but much less irregular than before the "new-spectra" update, compare upper left image before and after). The reason for nonlinearity is a contamination due to the influence of the interval below ~10 nm, which is not part of the 17-80 nm nominal interval of the Al channels. - Although the channel interval nominally reaches up to 80 nm, effectively it appears to end at 40 nm (see Figure 3-3). - For the small subset of flare events, the uncalibrated data of this channel (i.e. before subtraction of the substantial short-wavelength contamination) will probably not be very meaningful.

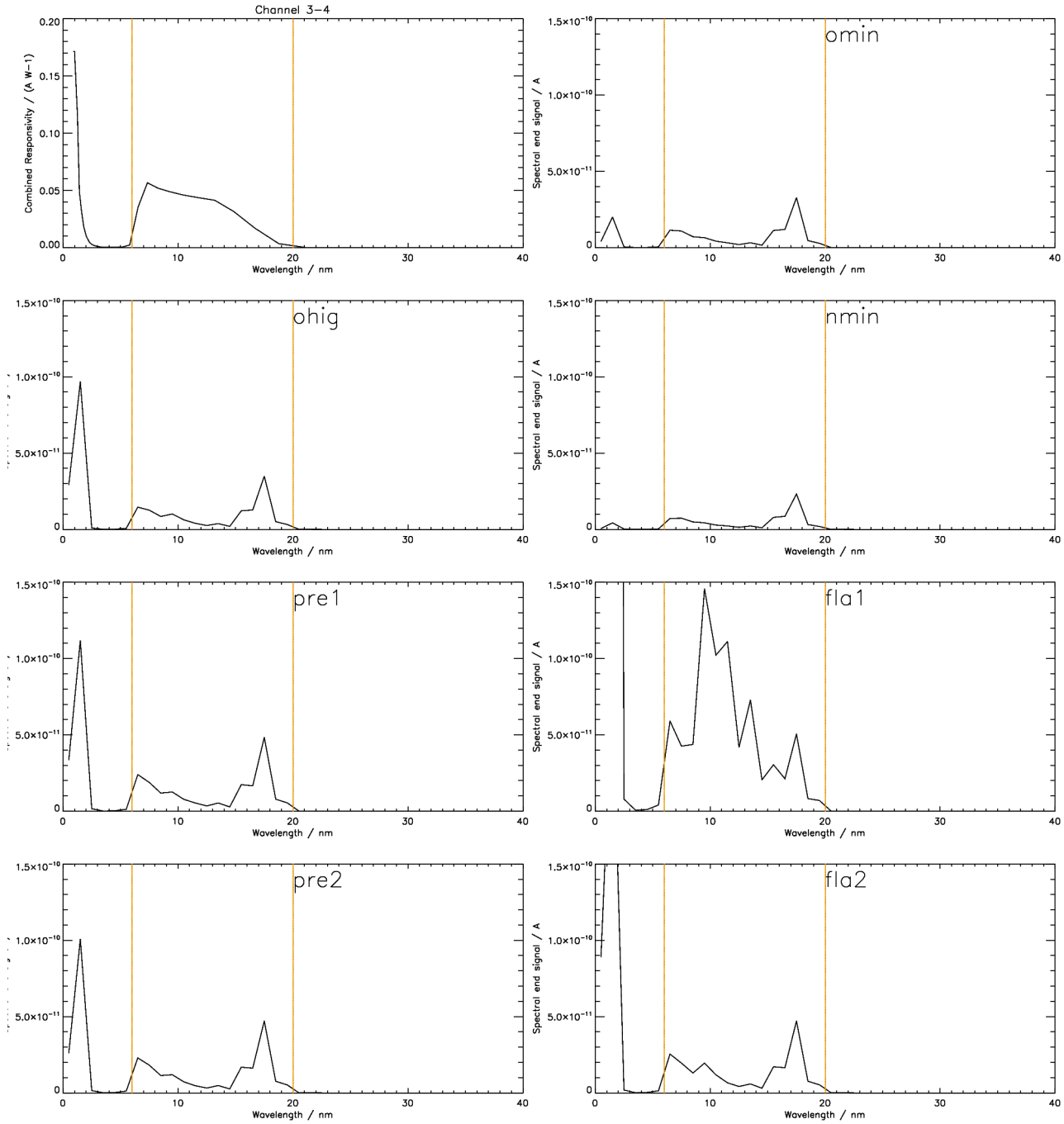

Figure 3-4. Measured responsivity and simulated output for LYRA channel 3-4
Zr(300nm) + AXUV20C (6-20 nm)

sample	total	pure	residual	solar
omin	0.142422 nA	0.113323 nA (79.6%)	0.0290983 nA	0.000889638 Wm-2
ohig	0.263439 nA	0.131955 nA (50.1%)	0.131484 nA	0.000996023 Wm-2
nmin	0.0871362 nA	0.0779099 nA (89.4%)	0.00922627 nA	0.000612958 Wm-2
pre1	0.339295 nA	0.187175 nA (55.2%)	0.152121 nA	0.00146242 Wm-2
fla1	5.37510 nA	0.757063 nA (14.1%)	4.61803 nA	0.00340528 Wm-2
pre2	0.313136 nA	0.179567 nA (57.3%)	0.133569 nA	0.00141076 Wm-2
fla2	0.567046 nA	0.202588 nA (35.7%)	0.364459 nA	0.00148986 Wm-2

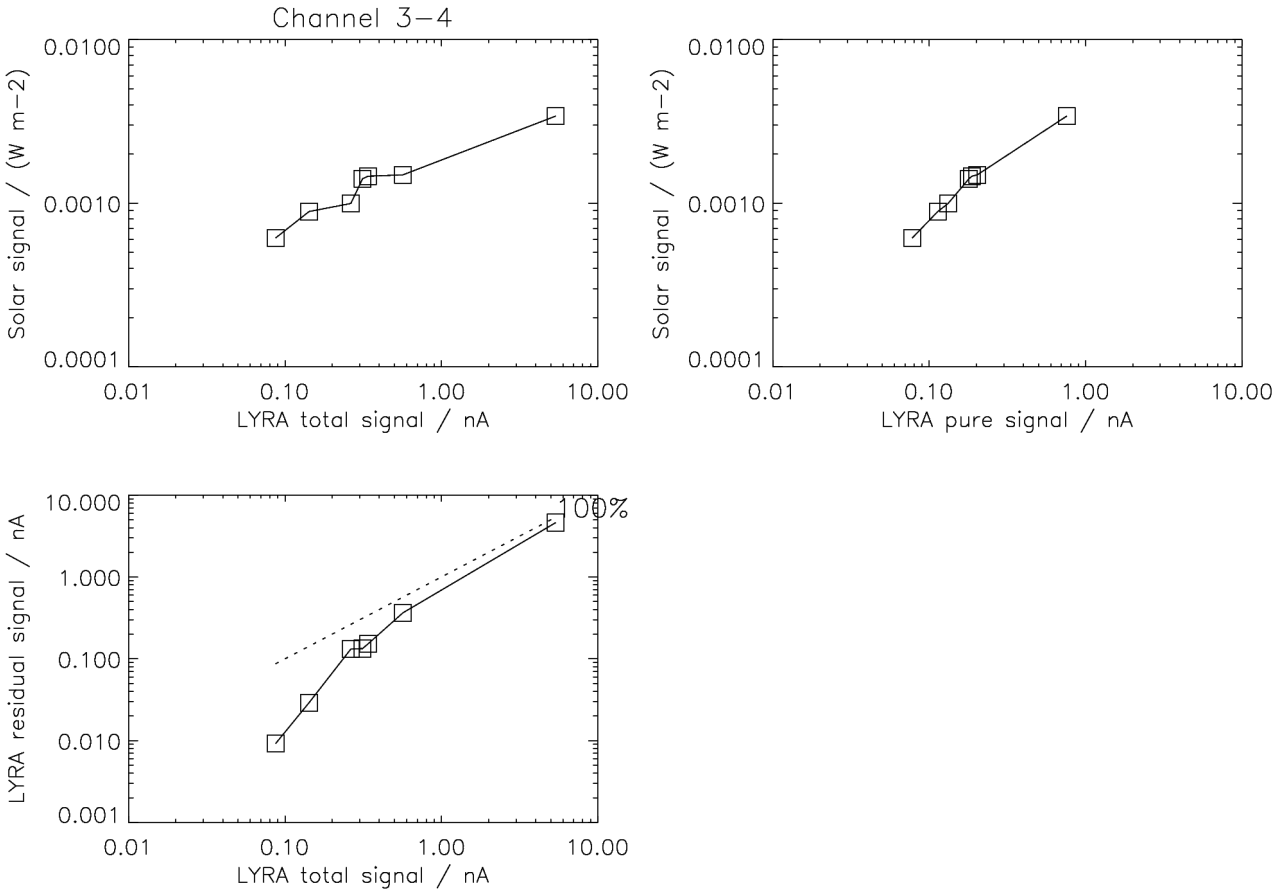

Figure 3-4a. Simulated relations between input and output for LYRA channel 3-4.

Remarks: After redefining the nominal interval of the Zr channel, the functional relation between the solar signal and the LYRA total signal is not straightforward any more, but rather resembles the Al channel. The reason for nonlinearity is a contamination due to the influence of the interval below ~3 nm, which is not part of the new 6-20 nm nominal interval of the Zr channels. - For the small subset of flare events, the uncalibrated data of this channel (i.e. before subtraction of the substantial short-wavelength contamination) will probably not be very meaningful.

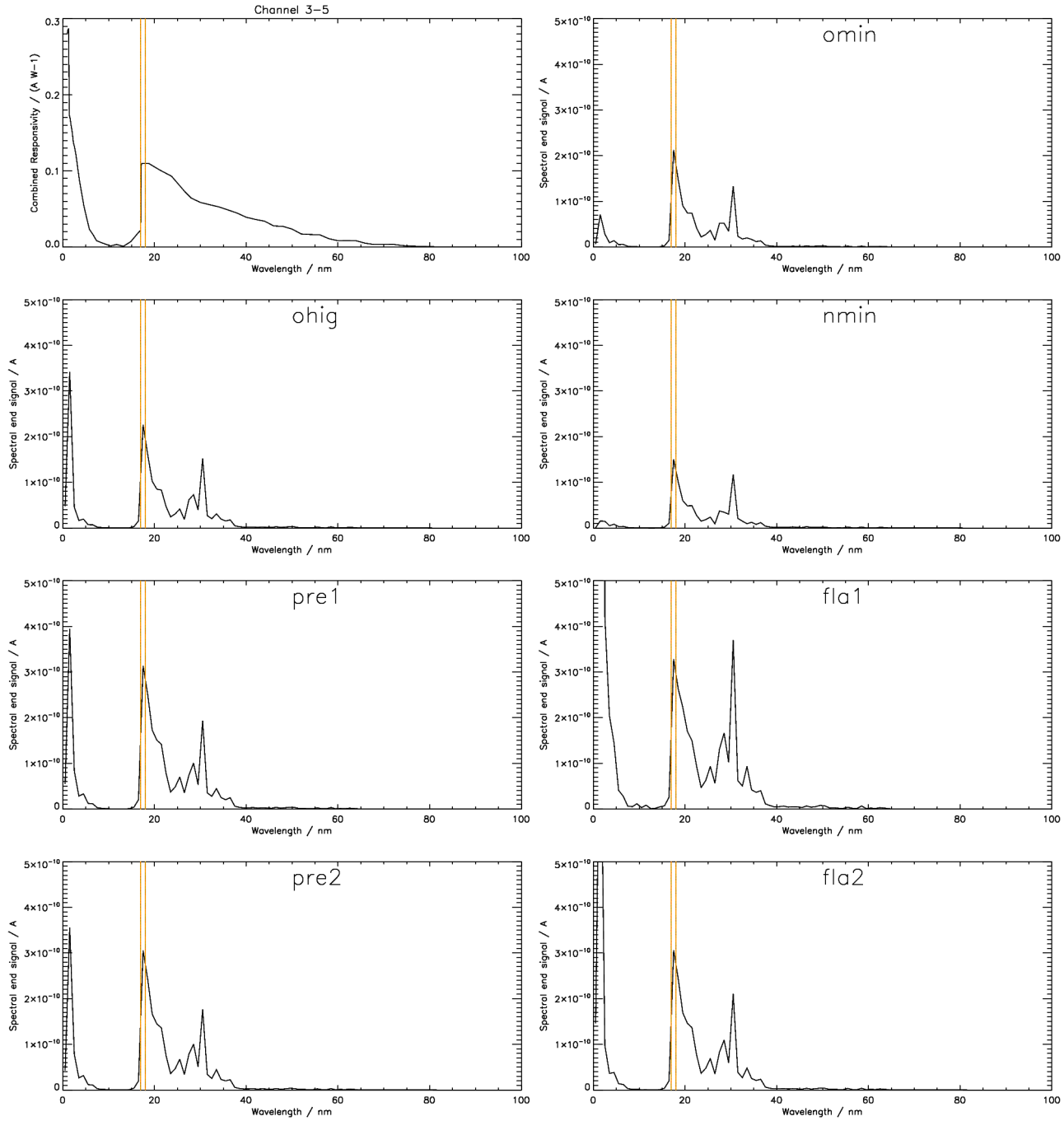

Figure 3-5. Measured responsivity and simulated output for the *virtual* LYRA channel 3-5 Aluminium + AXUV20B *(17-18 nm, for cross-calibration with SWAP)*

sample	total	pure	residual	solar
omin	1.32016 nA	0.212320 nA (16.1%)	1.10784 nA	0.000274049 Wm-2
ohig	1.83762 nA	0.225735 nA (12.3%)	1.61189 nA	0.000291364 Wm-2
nmin	0.906568 nA	0.150265 nA (16.6%)	0.756303 nA	0.000193953 Wm-2
pre1	2.61304 nA	0.313483 nA (12.0%)	2.29956 nA	0.000404624 Wm-2
fla1	16.7010 nA	0.328037 nA (2.0%)	16.3730 nA	0.000423409 Wm-2
pre2	2.47889 nA	0.305334 nA (12.3%)	2.17355 nA	0.000394106 Wm-2
fla2	3.30640 nA	0.306032 nA (9.3%)	3.00037 nA	0.000395006 Wm-2

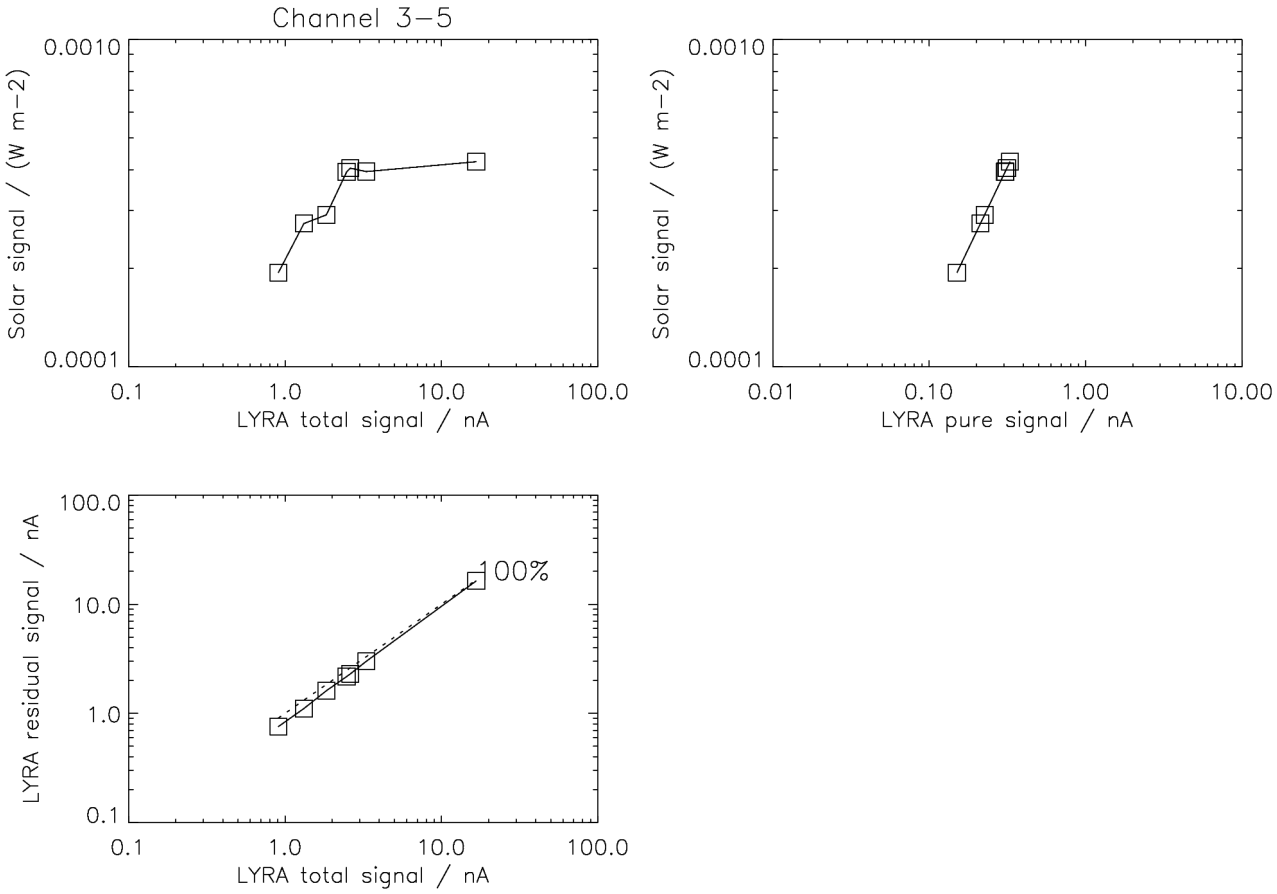

Figure 3-5a. Simulated relations between input and output for *virtual* LYRA channel 3-5.

Remarks: The functional relation between the (SWAP) solar signal and the LYRA total signal is not straightforward. One reason for nonlinearity is a contamination due to the influence of the interval below ~10 nm. It appears that a flare will hardly influence the solar irradiance as measured by SWAP.

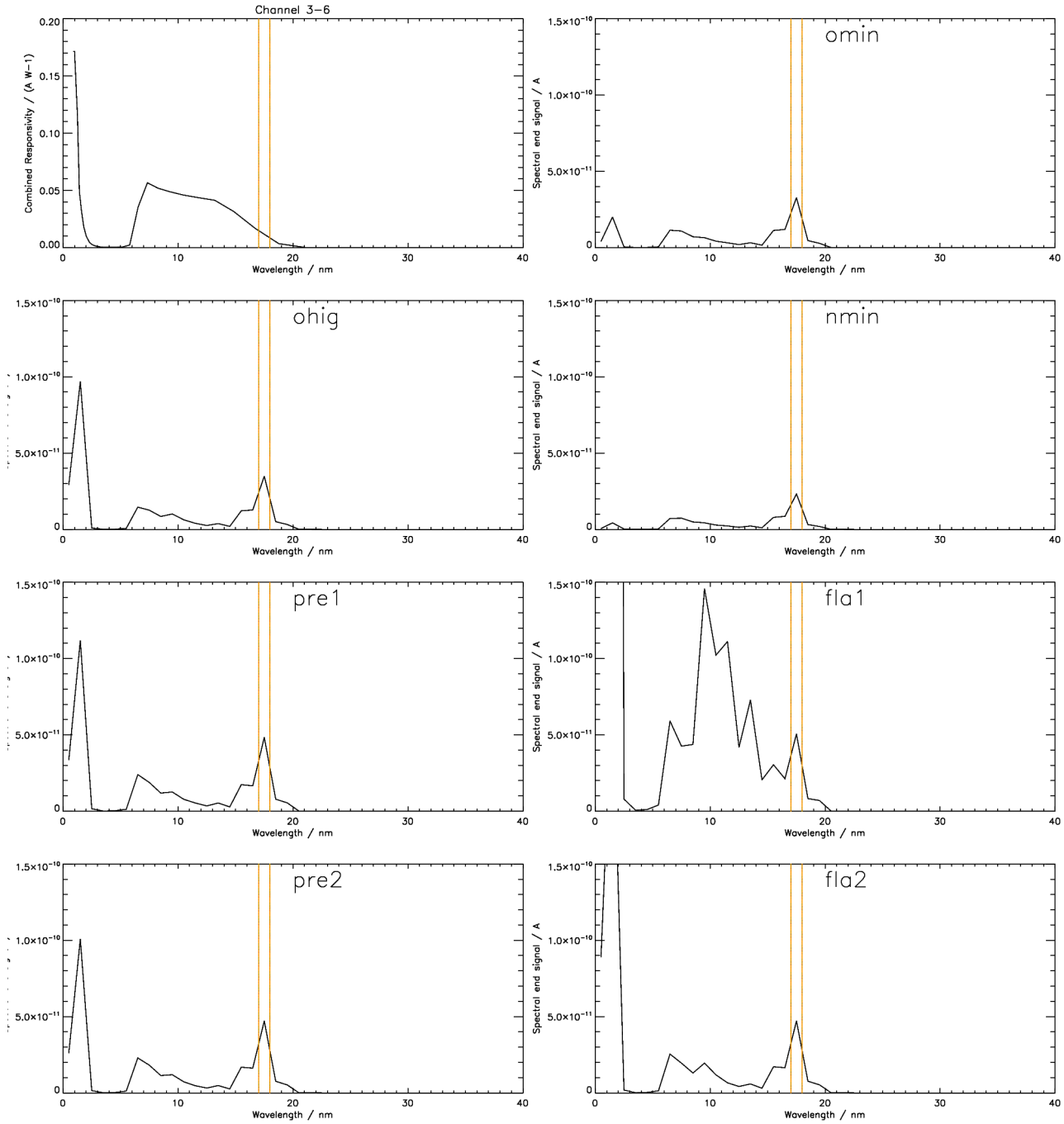

Figure 3-6. Measured responsivity and simulated output for the *virtual* LYRA channel 3-6 Zr(300nm) + AXUV20C *(17-18 nm, for cross-calibration with SWAP)*

sample	total	pure	residual	solar
omin	0.142422 nA	0.0327458 nA (23.0%)	0.109676 nA	0.000274049 Wm-2
ohig	0.263439 nA	0.0348147 nA (13.2%)	0.228624 nA	0.000291364 Wm-2
nmin	0.0871362 nA	0.0231752 nA (26.6%)	0.0639610 nA	0.000193953 Wm-2
pre1	0.339295 nA	0.0483480 nA (14.2%)	0.290947 nA	0.000404624 Wm-2
fla1	5.37510 nA	0.0505926 nA (0.9%)	5.32450 nA	0.000423409 Wm-2
pre2	0.313136 nA	0.0470912 nA (15.0%)	0.266045 nA	0.000394106 Wm-2
fla2	0.567046 nA	0.0471988 nA (8.3%)	0.519848 nA	0.000395006 Wm-2

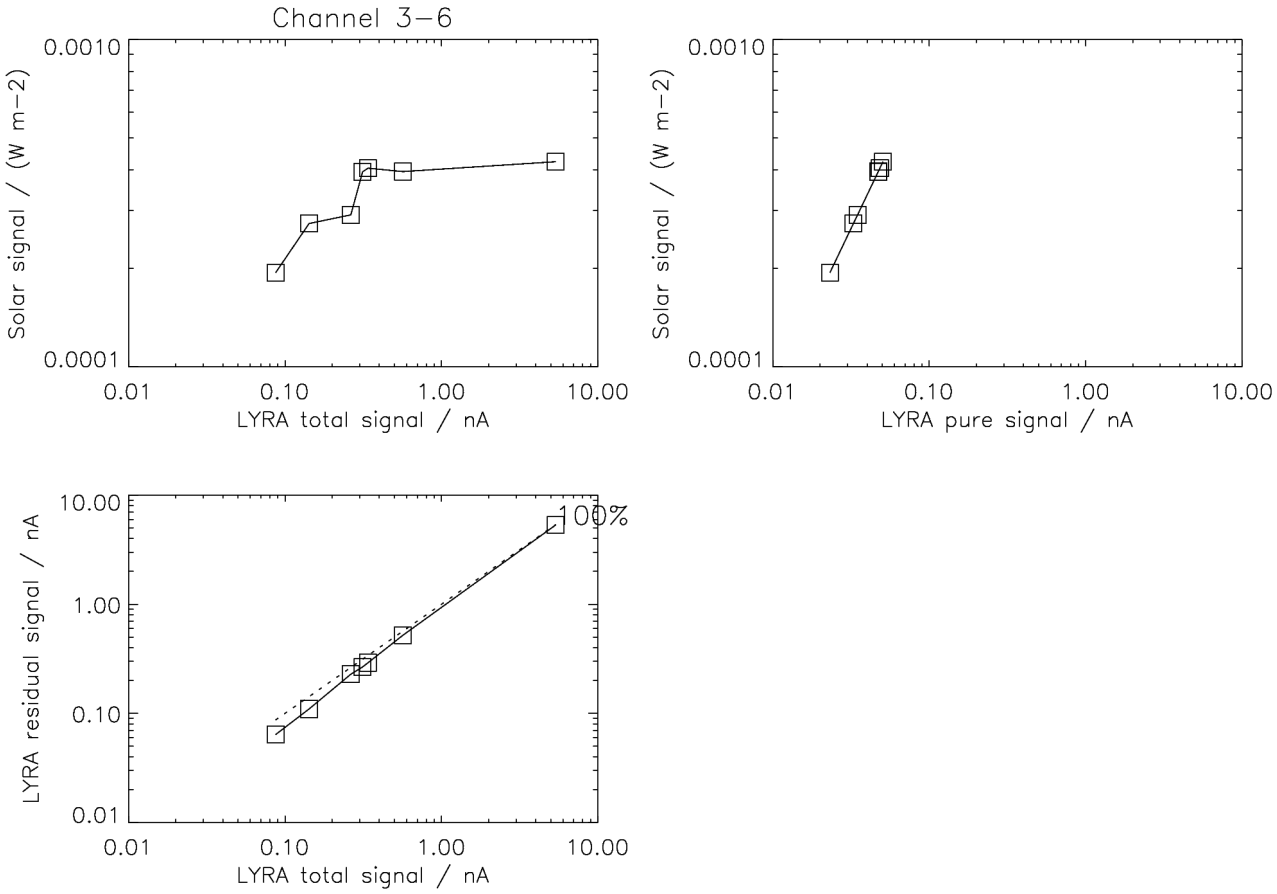

Figure 3-6a. Simulated relations between input and output for *virtual* LYRA channel 3-6.

Remarks: The functional relation between the (SWAP) solar signal and the LYRA total signal is not straightforward. One reason for nonlinearity is a contamination due to the influence of the interval below ~3 nm. It appears that a flare will hardly influence the solar irradiance as measured by SWAP.

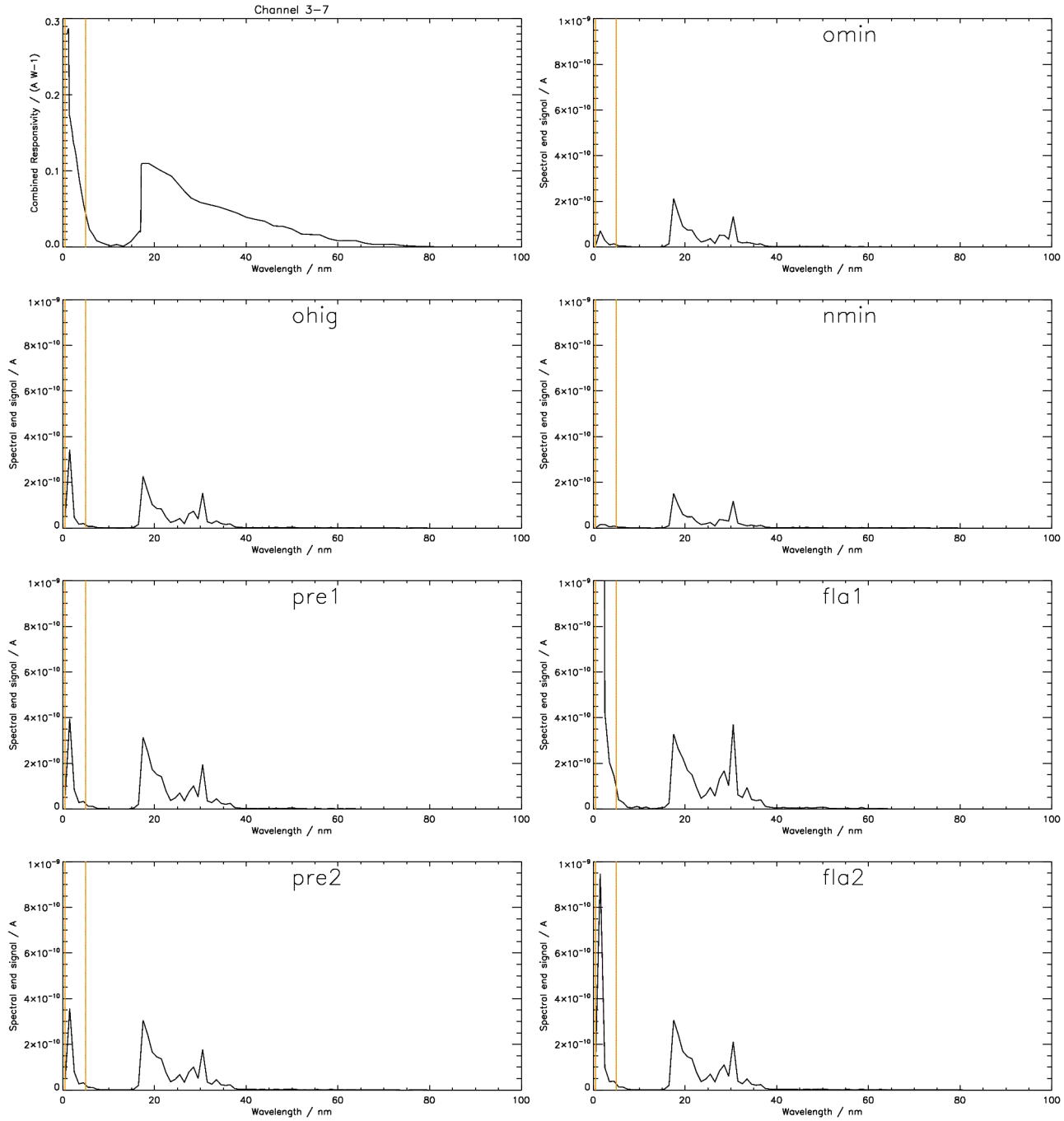

Figure 3-7. Measured responsivity and simulated output for the *virtual* LYRA channel 3-7
Aluminium + AXUV20B *(< 5 nm, for cross-calibration with TIMED/SEE, or additional product?)*

sample	total	pure	residual	solar
omin	1.32016 nA	0.128918 nA (9.8%)	1.19124 nA	0.000143220 Wm-2
ohig	1.83762 nA	0.470841 nA (25.6%)	1.36678 nA	0.000430065 Wm-2
nmin	0.906568 nA	0.0437577 nA (4.8%)	0.862811 nA	0.0000581368 Wm-2
pre1	2.61304 nA	0.593659 nA (22.7%)	2.01938 nA	0.000572517 Wm-2
fla1	16.7010 nA	13.8575 nA (83.0%)	2.84349 nA	0.0109987 Wm-2
pre2	2.47889 nA	0.534207 nA (21.6%)	1.94468 nA	0.000521914 Wm-2
fla2	3.30640 nA	1.26438 nA (38.2%)	2.04202 nA	0.00111161 Wm-2

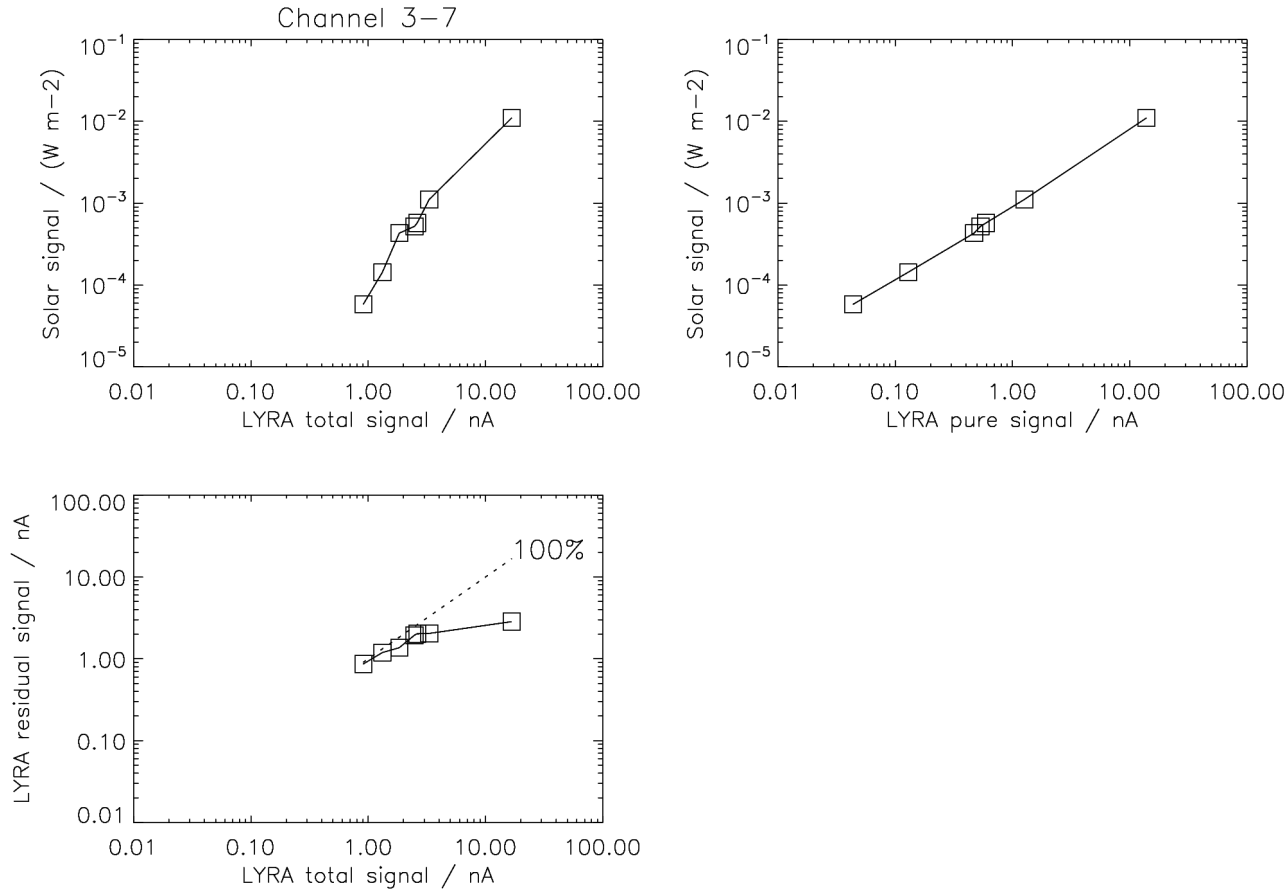

Figure 3-7a. Simulated relations between input and output for *virtual* LYRA channel 3-7.

Remarks: The functional relation between the (< 5 nm, SXR) solar signal and the LYRA total signal is not straightforward, because (a) the channel's responsivity is higher for short wavelengths, and (b) the EUV signal dominates in non-flare situations.

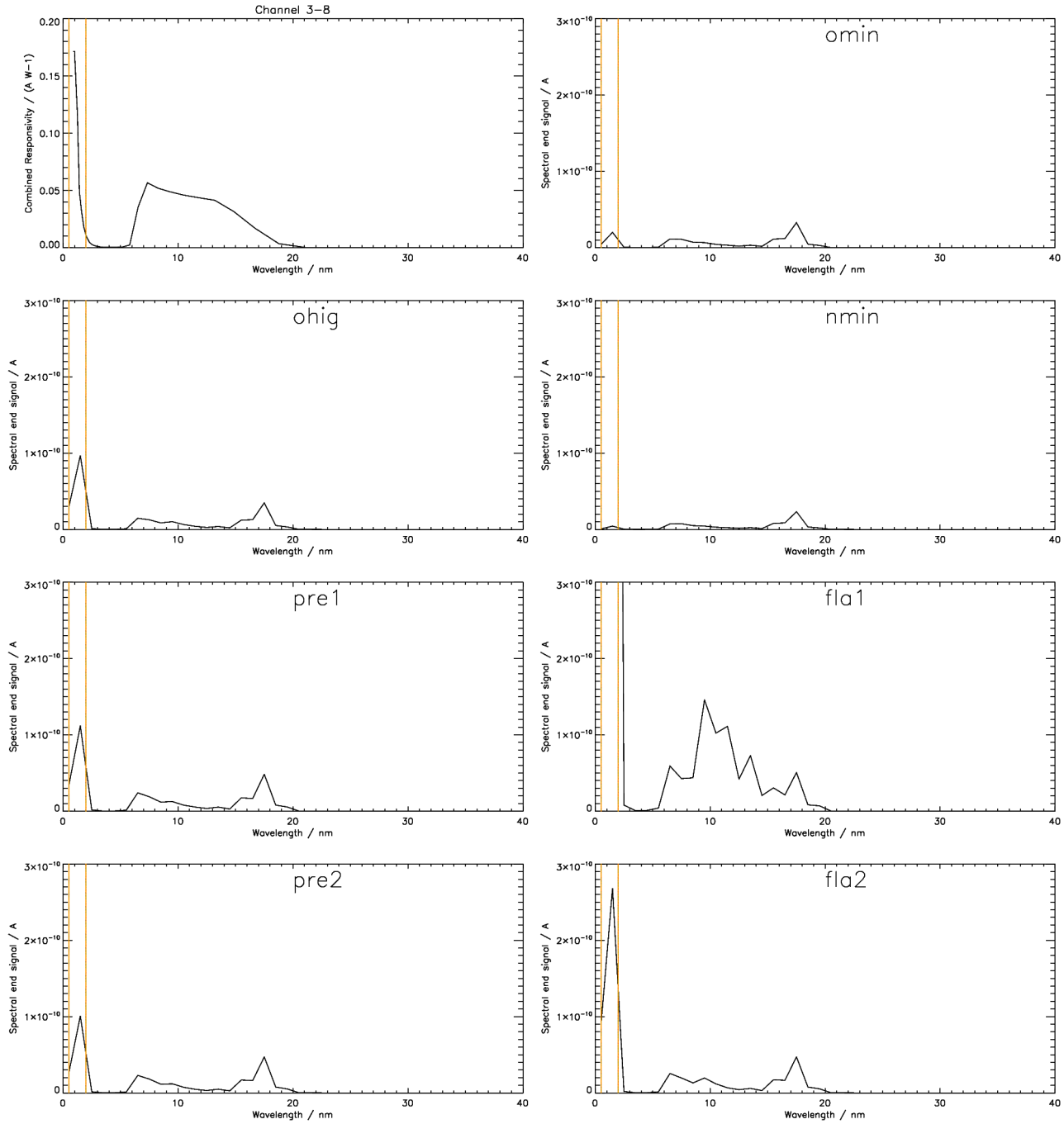

Figure 3-8. Measured responsivity and simulated output for the *virtual* LYRA channel 3-8
Zr(300nm) + AXUV20C *(< 2 nm, for cross-calibration with TIMED/SEE, or additional product?)*

sample	total	pure	residual	solar
omin	0.142422 nA	0.0241494 nA (17.0%)	0.118272 nA	0.0000611985 Wm-2
ohig	0.263439 nA	0.125961 nA (47.8%)	0.137478 nA	0.000303303 Wm-2
nmin	0.0871362 nA	0.0048156 nA (5.5%)	0.0823206 nA	0.0000127735 Wm-2
pre1	0.339295 nA	0.145184 nA (42.8%)	0.194111 nA	0.000350038 Wm-2
fla1	5.37510 nA	4.60069 nA (85.6%)	0.774408 nA	0.00983327 Wm-2
pre2	0.313136 nA	0.126798 nA (40.5%)	0.186337 nA	0.000312139 Wm-2
fla2	0.567046 nA	0.357056 nA (63.0%)	0.209990 nA	0.000846606 Wm-2

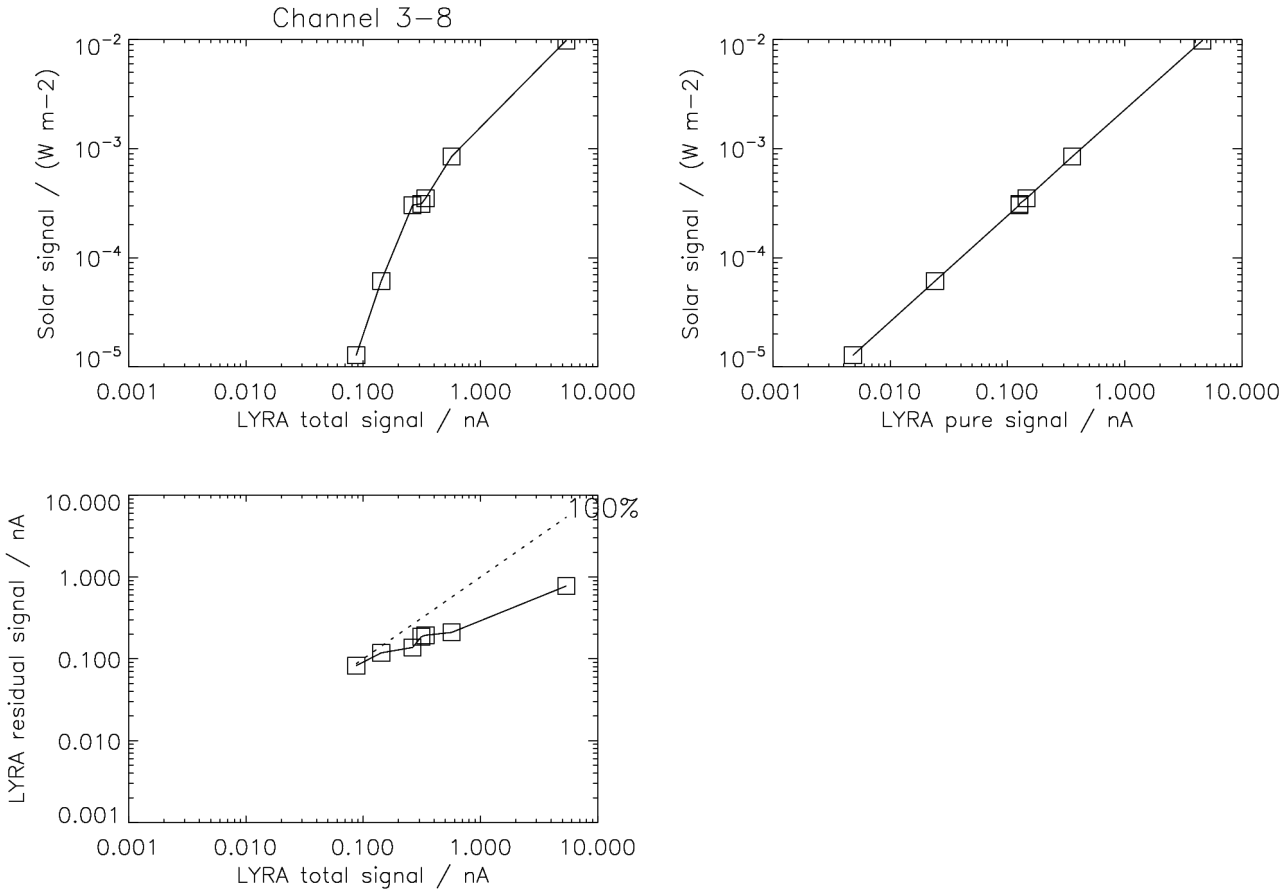

Figure 3-8a. Simulated relations between input and output for *virtual* LYRA channel 3-8.

Remarks: The functional relation between the (< 2 nm, SXR) solar signal and the LYRA total signal is not straightforward, because (a) the channel's responsivity is higher for short wavelengths, and (b) the EUV signal dominates in non-flare situations.